Aus dem Institut für Biochemie und Molekularbiologie II
der Heinrich-Heine-Universität Düsseldorf
Direktor:
Univ.-Prof. Dr. Jürgen Scheller

Investigating the expression and role of embryonic stem cell-expressed RAS (ERAS) in human cancer cells

Dissertation

zur Erlangung des Grades eines Doktors der Medizin
der Medizinischen Fakultät der Heinrich-Heine-Universität Düsseldorf

vorgelegt von

Inga Rebecca Heinen

2021

Als Inauguraldissertation gedruckt mit der Genehmigung der
Medizinischen Fakultät der Heinrich-Heine-Universität Düsseldorf

gez.:
Dekan: Prof. Dr. med. Nikolaj Klöcker
Erstgutachter: Prof. Dr. rer. nat. Reza Ahmadian
Zweitgutacher: Prof. Dr. med. Guido Reifenberger

Abstract

Embryonic stem cell-expressed RAS (ERAS) is a novel member of the RAS protein family. ERAS has first been detected in undifferentiated embryonic stem cells of mice and later in defined human cancer cell lines, such as gastric, neuroblastoma, breast, pancreatic and colorectal cancers, and very recently also in hepatic stellate cells of rats. It was shown that ERAS holds critical functions for the maintenance of the quiescent properties of the hepatic stellate cells. However, the function of ERAS in cancer cells is not studied in detail and needs further investigation. Unlike other RAS proteins, ERAS is constitutively active and its activity is most probably regulated at the transcription level. Therefore, the focus of this study was the identification of the human cell lines, which express *hs*ERAS. Expression analysis of *hs*ERAS at the mRNA level was, therefore, analyzed in detail in colorectal (DLD1, HCT116, HT29, LOVO, SW480), pancreatic (CAPAN1, CAPAN2, MIA PaCa2), prostate (BPH-1, PNT-2), teratocarcinoma (NCCIT, Tera-1, Tera-2, NT-2), neuroblastoma (SH-SY5Y, IMR-32) and glioblastoma (U87MG, A172) cell lines. This was conducted by qPCR with a validated set of primers. For the first time, such a wide range of human cancer entities was investigated concerning the expression of *hs*ERAS. This study shows that especially the teratocarcinoma cells (Tera-1, Tera-2 and NT-2) and the neuroblastoma cells (IMR-32 and SY-SY5Y) have significantly high levels of *hs*ERAS mRNA. To determine ERAS at the protein level in these cells by immunoblot analysis, an anti-*hs*ERAS antibody, which specifically detects the N-terminus of ERAS, was validated using various RAS proteins purified from *Escherichia coli* and produced in COS-7 cell line. However, comprehensive protein analyses in this study clearly pointed out that there is no detectable ERAS protein in the respective tumor cell lysates. The reason for ERAS not being translated is still unclear and therefore, further investigations are necessary.

Zusammenfassung

Embryonic stem cell-expressed RAS (ERAS) ist ein neuartiges Mitglied der RAS-Proteinfamilie. ERAS wurde zunächst in undifferenzierten embryonalen Stammzellen von Mäusen und später in definierten menschlichen Krebszelllinien wie Magen-, Neuroblastom-, Brust- , Bauchspeicheldrüsen- und Darmkrebs sowie in jüngster Zeit auch in hepatischen Sternzellen der Ratte nachgewiesen. Es wurde gezeigt, dass ERAS kritische Funktionen für die Aufrechterhaltung des Ruhezustandes der hepatischen Sternzellen hat. Die Funktion von ERAS in Krebszellen ist jedoch nicht im Detail bekannt und bedarf weiterer Untersuchungen. Im Gegensatz zu anderen RAS-Proteinen ist ERAS permanent aktiv. Diese Aktivität wird höchstwahrscheinlich auf der Transkriptionsebene reguliert. Daher lag der Schwerpunkt dieser Arbeit auf der Identifizierung der menschlichen Zelllinien, die hsERAS exprimieren. Die Expressionsanalyse von hsERAS auf mRNA-Ebene wurde deshalb im Detail in Dickdarmtumorzelllinien (DLD1, HCT116, HT29, LOVO, SW480), Bauchspeicheldrüsentumorzelllinien (CAPAN1, CAPAN2, MIA PaCa2), Prostatazelllinien (BPH-1, PNT-2), Teratokarzinomzelllinien (NCCIT, Tera-1, Tera-2, NT-2), Neuroblastomzelllinien (SH-SY5Y, IMR-32) und Glioblastomzelllinien (U87MG, A172) durchgeführt. Dies wurde mittels qPCR mit einem validierten Satz von Primern vorgenommen. Zum ersten Mal wurde ein so breites Spektrum an menschlichen Krebsarten hinsichtlich der Expression von hsERAS untersucht. Diese Arbeit zeigt, dass vor allem die Teratokarzinomzellen (Tera-1, Tera-2 und NT-2) und die Neuroblastomzellen (IMR-32 und SY-SY5Y) einen signifikant hohen Gehalt an hsERAS mRNA aufweisen. Um ERAS auf Proteinebene in diesen Zellen mittels Immunoblotanalyse zu bestimmen, wurde ein anti-hsERAS-Antikörper, der spezifisch den N-Terminus von ERAS nachweist, mit verschiedenen RAS-Proteinen validiert, die sowohl aus *Escherichia coli* gereinigt und als auch in der COS-7-Zelllinie produziert wurden. Die umfassende Proteinanalyse in dieser Arbeit hat jedoch deutlich gezeigt, dass in den jeweiligen Tumorzelllysaten kein nachweisbares ERAS-Protein vorhanden ist. Der Grund für die mangelnde Translation von ERAS ist noch unklar, so dass weitere Untersuchungen erforderlich sind.

Abbreviations

aa	aminoacid
A / Ala	alanine
Amp	ampicillin
APS	ammonium persulphate
AB	antibody
Bp	base pairs
c	concentration
C / Cys	cysteine
cDNA	complementary DNA
°C	degree centigrade
C-Terminus	carboxy-terminus
CT	cycle threshold
D / Asp	aspartic acid
ddH_2O	double distilled water
DMEM	Dulbecco's modified eagle medium
DMSO	dimethyl sulfoxide
DNA	deoxyribonucleic acid
DTT	dithiothreitol
E / Glu	glutamic acid
E. coli	escherichia coli
F / Phe	phenylalanine
FBS	fetal bovine serum
Fig.	figure

fl	full-length
FW	forward
G / Gly	glycine
GAPs	GTPase-activating proteins
GDP	guanosine diphosphate
GEFs	guanine nucleotide exchange factors
GSH	reduced Glutathione
GST	glutathione S-transferase
GTP	guanosine triphosphate
GTPases	guanosine triphosphatase
h	hour
H / His	histidine
HRP	horseradish peroxidase
I / Ile	isoleucine
IPTG	isopropyl β-D-1-thiogalactopyranoside
K / Lys	lysine
kDa	kilodalton
L	liter
L / Leu	leucine
M / Met	methionine
MAPK	mitogen-activated protein kinase
mg	milligram
min	minute
ml	milliliter
mM	millimolar

mRNA	messenger RNA
MW	molecular weight
N / Asn	asparagine
NaCl	sodium chloride
ng	nanogram
nm	nanometer
ORF	open reading frame
P / Pro	proline
PCR	polymerase chain reaction
PD	pull-down
P/S	Penicillin/ Streptomycin
Q / Gln	glutamine
R / Arg	arginine
RAS	rat sarcoma
RBD	Rho-binding domain
RHO	Ras homologues
RNA	ribonucleic acid
rpm	rounds per minute
RT	room temperature
RV	reverse
S / Ser	serine
SDS	sodium dodecyl sulfate
SDS-PAGE	sodium dodecyl sulfate polyacrylamide gel electrophoresis
sec	second
T / Thr	threonine

TEMED	tetramethylethylenediamine
U	unit
U / Sec	selenocysteine
V	volume
V / Val	valine
W / Trp	tryptophan
Y / Tyr	tyrosine
µg	microgram
µl	microliter
µM	micromolar
%	percent

Table of Contents

Table of Figures

Chapter 1

1.1 Carcinogenesis

Cancer is a disease which takes a huge role in the society worldwide. It is not only the second leading cause of death in the United States (Siegel, Miller, & Jemal, 2019) but also one of the leading causes of death worldwide (Bray, 2014). The reasons for the outbreak of cancer are varied and often not well known. In healthy organisms, cell growth and cell division are precisely and well controlled. Damage of the DNA, concerning genes that control cell growth, cell division, apoptosis and differentiation, can lead to the development of cancer (Hanahan & Weinberg, 2000). This development is a very complex multistep process called carcinogenesis. During this process several somatic mutations in different genes within a cell accumulate (multi-hit concept) (Vogelstein & Kinzler, 1993). As a consequence, the degenerating cells acquire in the course of the carcinogenesis six biological capabilities belonging sustaining proliferative signaling, passing from the cell cycle check points, inducing angiogenesis, resisting cell death, enabling replicative immortality and activating invasion and metastasis (Hanahan & Weinberg, 2000). This process takes several years and is divided into different phases including the initiation, the promotion, and the progression (Barrett, 1993).

Initiation

The initiation describes the beginning of the carcinogenesis (Fig. 1). During this phase carcinogenic agents result in DNA damages and therefore increase the rate of genomic mutations during DNA repair responses (Yuspa & Poirier, 1988). Mutations in genes participating the processing of signaling pathways concerning cell growth, proliferation and apoptosis are known for inducing the degeneration of cells and thus the carcinogenesis (Hanahan & Weinberg, 2011). Generally, mutations in two classes of genes show great promise in the development of cancer. On the one hand the so-called proto-oncogenes coding for proteins controlling cell growth and cell division and on the other hand the tumor-suppressor genes coding for proteins inhibiting these processes. The activation or upregulation of oncogenes and the inactivation of tumor-suppressor genes are key players in the tumor initiation and progression. Cancer-related mutations of proto-oncogenes result in increased activity of the gene product and in a gain of function. Very well-known proto-

oncogenes are *RAS* genes. Almost 30% of human cancers contain mutation within the *RAS* genes. Point mutations are frequently found in three critical codons G12, G13 and Q61 leading to hyper-activation of the RAS proteins and consequently to uncontrolled cell signaling (See **Biological functions of the RAS proteins** and **The role of RAS proteins in carcinogenesis**). 90 % of the pancreatic carcinoma, 50 % of the colorectal carcinoma and 30 % of lung cancer show *RAS* mutations. This makes the RAS gene the most widely activated oncogene in human cancers (Bertram, 2000) (Hanahan & Weinberg, 2011). However, somatic mutations in tumor-suppressor genes result in a loss of function due to inactivation of these genes (Bertram, 2000). Mutations of two main tumor-suppressor genes are well known: p53 (TP53) is known as "the guardian of the genome"(Lane) and APC (Adenomatous-polyposis-coli) take a central role in the initiation of colorectal carcinogenesis (Weinberg, 2014). They enhance tumor formation and progression together with oncogenic RAS mutations. Although TP53 is the generally best-known tumor-suppressor gene, it rather takes a role during the tumor progression. While mutation of only one allele leads to the activation of proto-oncogenes, mutation of both alleles of tumor-suppressor genes is required for tumor initiation. Thus, proto-oncogenes behave dominant and tumor-suppressor genes recessive (Bertram, 2000). Mutations resulting in the development of cancer do not only occur in somatic cells, but also in germline cells. These germline mutations resulting in hereditary cancer development helped characterize the role of tumor-suppressor genes in carcinogenesis. An example for this is the Li-Fraumeni syndrome. Patients suffering from this syndrome most frequently exhibit a germline mutation of TP53 (Malkin et al., 1990).

However, initiation of carcinogenesis does not only underlie genetic causes, but also epigenetic alterations are known to induce activation of oncogenes and inactivation of tumor-suppressor genes (Peltomaki, 2012).

Promotion

The proceeding of the carcinogenesis is described as promotion. In this phase, initiated cells proliferate and form a benign tumor, consisting of so-called preneoplastic cells. These cells do not have any malignant properties and can be distinguished with regard to morphology, invasiveness, growth and differentiation from neoplastic cells. They, furthermore, react differently to chemical treatments when compared to the malignant cells (Barrett, 1993).

Various biological and biochemical mechanisms are responsible for the tumor promotion that are either toxic or mitogenic. Some chemical agents, termed tumor promoters, are known to be cytotoxic for specific populations of cells causing their proliferation. Proliferating cells are at risk of accumulating further mutations. A representative example is the consumption of cigarettes and alcohol. The tobacco tar contained in cigarettes is an already known initiating agent and consumption of promoting alcohol can additionally lead to aggressive head-and-neck cancer for example. However, noted mitogenic agents are steroid hormones. Estrogen, therefore, induces the proliferation of initiated mammary epithelial cells. However, the greatest tumor promoter seems to be inflammatory processes (Weinberg, 2014). Several murine models have affirmed that inflammatory processes promote cancer development. Chronic infections with *Helicobacter pylori* promote gastric carcinoma and MALT lymphoma. Patients infected with Hepatitis B or C can develop hepatocellular carcinoma (Balkwill, Charles, & Mantovani, 2005). The clonal expansion of initiated cells is necessary for the progression of the tumor and thus for the transformation to malignant cells: Initiated cells do not exhibit abilities that malignant cells possess. Therefore, further mutations are necessary and proliferation by clonal expansion of initiated cells both increases the probability of additional mutations and leads to a higher replication rate. This leads to miscopied DNA, and increases cell division rate that can come along with chromosomal aberrations (Weinberg, 2014).

Transformation

Transformation is less a phase than a process itself, representing the degeneration of a normal cell to a malignant cell harboring cancer-specific ability. As mentioned above, clonal expansion is a prerequisite for the transformation of cells and is ensured by promoters-like agents (*i.e.* alcohol) and inflammation. Therefore, a regular exposure to the promoter agent is more critical than a high dose of it. Once the promoter is deprived of the system, the benign tumor can regress. However, when the cells transformed to malignant cells regression of the tumor holds off even after the exposure to the promoter is halted (Weinberg, 2014).

Progression

During the tumor progression the cells forming the benign lesion accumulate more mutations and epigenetic alterations, leading to a malignant phenotype (Barrett, 1993) (Weinberg,

2014). Thus, the cells acquire cancer-typical abilities belonging sustaining proliferative signaling, passing from the cell cycle check points, inducing angiogenesis, resisting cell death, enabling replicative immortality and activating invasion and metastasis (Hanahan & Weinberg, 2011). However, the tumor progression proceeds rarely because of repair mechanisms (Bertram, 2000) (Weinberg, 2014). Furthermore, the progression is likely to take less time than the previous phases since the cells have already have accumulated a series of mutations and thus also acquired abilities to proliferate uncontrolledly. As already mentioned mutations within oncogenes and tumor-suppressor genes also appear during the tumor progression. Mutations of TP53 are likely to appear during the progression of colorectal carcinoma, but are also found in tumors of various tissue types, such as pancreas, lung, breast and brain (Hollstein, Sidransky, Vogelstein, & Harris, 1991). As a transcription factor TP53 is involved in regulating cell cycle arrest, apoptosis and DNA repair. Its mutations occur in more than 50 % of human cancers (Bertram, 2000) (Carrier et al., 1999).

Invasion and Metastasis

A typically dreaded characteristic of cancer is the invasion and the metastasis of malignant cells in adjacent tissue in the entire human body. As already described above, only malignant cells exhibit this capability. Metastasis is a complex cascade of different steps. For this process angiogenesis is essential. The tumor cells need to leave the primary tumor through the basement membrane, which is possible by dissolution of the membrane and following cell locomotion. Consequently, the cells have need to invade the adjacent tissue, and nonetheless enter blood or lymphatic vessels. Moreover, the tumor cells must survive the journey through the blood/lymphatic system since it is enriched with immune cells. After extravasation, the malignant cells have to be able to build up a secondary tumor in a new tissue. Less than 0.01 % of the circulating tumor cells survive this journey. However, genetic changes, causing uncontrolled proliferation, are not sufficient for this process (Liotta & Stetler-Stevenson, 1991). A drastic change of the phenotype is necessary, which is represented by an epithelial-mesenchymal transition (EMT), going along with a different genetic expression pattern. Accordingly, the expression of cytokeratins and E-cadherin, which are actually fundamental components of epithelial cells, is downregulated, and expression of vimentin, a component of mesenchymal cells, is upregulated. Interestingly, EMT is not necessarily a pathological process: EMT physiologically happens during embryogenesis, *i.e.* during gastrulation when ectodermal cells start to form the mesoderm.

Amongst other things, this indicates that the expression pattern of invasive cells depends on the reactivation of the expression pattern found in stages of embryogenesis. This way of thinking consequently means that carcinoma cells do not acquire the ability to invade and metastasize step by step, they rather reactivate a program that was always encoded in their genome (Weinberg, 2014).

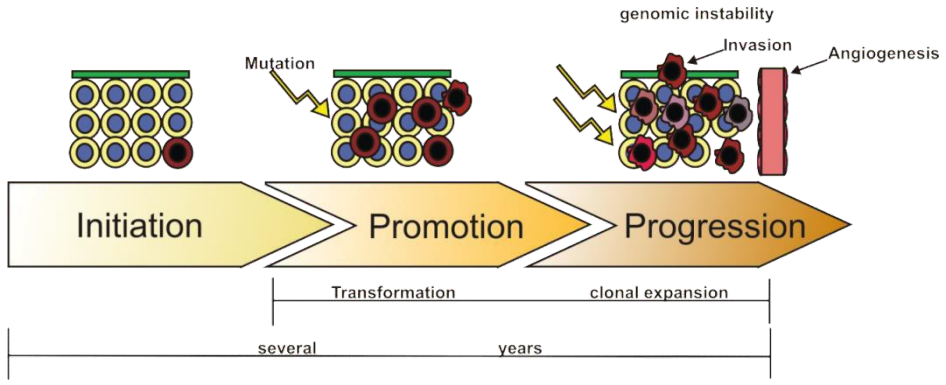

Figure 1: Multistep carcinogenesis.
Scheme of the multistep carcinogenesis illustrates the different steps of initiation, promotion and progression in which the cells acquire the associated properties of cancer. For further details, see the text. Adapted from (Liu et al., 2015).

1.2 Classification of tumors and introduction to the cell lines

An international standardized classification was elaborated by the WHO and the UICC (Union for International Cancer Control) to make discussions easier worldwide regarding the cancer type and stage as well as the therapeutic options the patients have (Table. 1). This classification incorporates the aspects "typing", meaning the determination of the tissue-origin of the tumor cells. Furthermore, it also includes "staging", and "grading". For the staging the TNM-formula was designed by the UICC, which consists of mainly three letters: "T" stands for the **t**umor size (meant is the primary tumor), "N" for the lymph **n**odes being infiltrated by cancer cells, and "M" for **m**etastasis in other organ systems. But as the type of degenerated tissue and the stage of the tumor is not sufficient to classify a cancer in order to treat the patient, a grading is necessary, too. Therefore, the histological conformity of the tumor with its tissue of origin is determined. There are four categories: G1 means that the cancer cells are highly differentiated and thus similar to their tissue of origin, whereas G4 means that the cancer cells are dedifferentiated and have no conformity to their tissue of origin. Thus, the classification comprises information being important not only to estimate the prognosis of the patient, but also to decide about the therapeutic options. Principally cells

which are not differentiated anymore tend to grow faster and are highly malignant (Riede, Werner, & Freudenberg, 2009).

Table 1: Nomenclature of some solid tumors according to their tissue type

Tissue type	Benign tumor	Malignant tumor
epithelia	aglanular: papilloma glandular: adenoma	aglandular: carcinoma glandular: adenocarcinoma
connective	-oma (fibroma)	-sarcoma (fibrosarcoma)
supportive connective	-oma (*i.e.* osteoma)	-sarcoma (*i.e.* osteosarcoma)
muscles	skeletal: rhabdomyoma smooth: leiomyoma	skeletal: rhabdomyosarcoma smooth: leiomyosarcoma

The gray marked tumors were investigated in this work. Please note that not all types of tumors are listed.

1.3 The RAS family of small GTPases

An overview of the RAS superfamily

The human RAS superfamily of small guanosine triphosphatases (GTPases) consists of more than 150 monomeric G protein members. According to the structural and functional features of the proteins, this protein superfamily is divided into five different families, including RAS, RHO, RAB, ARF and RAN. However, all these proteins contain a highly-conserved domain, so-called G domain, which consists of five motifs, including effector binding domain so called, Switch I (G2) and Switch II (G3) (Fig. 3). These motifs allow the RAS proteins to function as efficient molecular switches and therefore to take a crucial role in the signaling of the cell (Wennerberg, 2005). Here, we mainly focus on the RAS family.

Regulation and biological functions of RAS proteins

RAS proteins serve as molecular switches, cycling between two states: a GTP-bound active and a GDP-bound inactive state (Wittinghofer & Vetter, 2011). As a GTPase enzyme they are able to hydrolyze GTP to GDP and inorganic phosphate. However, the intrinsic rate of GTP hydrolysis is very low and thus they need acceleration which is given by so called GTPase activating proteins (GAPs)(Ahmadian, Hoffmann, Goody, & Wittinghofer, 1997; Bourne, Sanders, & McCormick, 1991; Scheffzek et al., 1997). Furthermore, exchange of

GDP for GTP and so the activation of the RAS proteins needs to be accelerated by Guanine nucleotide exchange factors (GEFs)(Buday & Downward, 2008; Wennerberg, 2005). While these two mechanisms are common for all of the RAS proteins, each family possess its specific GEFs and GAPs (Bishop & Hall, 2000). Only in their GTP-bound forms they interact with downstream effector proteins. Depending on the type of the extracellular signals they activate a distinct effector protein, and thereby regulate various processes in the cell, such as metabolism, cell cycle progression, proliferation, survival and the cell motility (Coleman, Marshall, & Olson, 2004). Not only somatic but also germline mutations in RAS family members and their signaling components are known as triggers for developmental disorders, such as Noonan syndrome and cardiac defects (Cirstea et al., 2013; Cirstea et al., 2010; Flex et al., 2014; Gremer et al., 2011).

Lipid modifications

RAS proteins are commonly known as membrane localized proteins. Their association with the membranes is mediated by posttranslational modification (PTM) of a region in the C-terminus, called hyper-variable region (HVR). Two different regions at the C-terminus are concerned by the lipid modification: I) The so-called *CAAX* motif (C= cysteine, A= aliphatic amino acid, X= any other amino acid) and II) one or two cysteines upstream of the *CAAX* motif (Cho et al., 2012). This modification leads to an enrichment of RAS proteins at the plasma membrane and therefore increases the efficiency of RAS signaling (Schmick et al., 2014).

The RAS subfamily

The first described proteins of the RAS family are the rat sarcoma (RAS) proteins, therefore, known as the founding members of this protein family (Repasky, Chenette, & Der, 2004). HRAS, NRAS and KRAS are well-investigated RAS members. Their activation affects the cell proliferation, differentiation and apoptosis. Despite their common functions, these proteins show different expression patterns, regulations and localizations within the cell (Castellano & Santos, 2011; Omerovic, Laude, & Prior, 2007; Potenza et al., 2005). Among different members of this family, some functions of a novel RAS family member, the embryonic stem cell-expressed RAS (ERAS), have been recently described in rat hepatic stellate cells (Nakhaei-Rad et al., 2016; Nakhaei-Rad et al., 2015). However, the role of ERAS in human cells remain unclear and need to be investigated.

1.4 The role of RAS proteins in carcinogenesis

As already mentioned, RAS proteins take crucial roles in intracellular cell signaling and are involved in cellular processes such as cell proliferation, differentiation and apoptosis (Castellano & Santos, 2011). Consequently, oncogenic activation of the RAS genes, their regulators and signaling components lead to dysregulation of the cell and the development of cancer. Mutation of three common RAS genes, HRAS, NRAS and KRAS4B (an alternative splice variant of KRAS), are found in several human cancer entities such as pancreatic, colon, lung cancer and leukemia (Castellano & Santos, 2011; Pylayeva-Gupta, Grabocka, & Bar-Sagi, 2011). Whereas KRAS mutations especially occur in pancreatic (>90%) (Waters & Der, 2018) but also in colon and lung cancer, NRAS mutations rather occur in leukemia (10%), and HRAS mutations are found in skin, head and neck cancer (Castellano & Santos, 2011; Pylayeva-Gupta, et al., 2011) (Fig. 2).

RAS mutations- germline and somatic mutations of RAS and its signaling components trigger several human developmental disorders and cancer, respectively (Gremer, et al., 2011). Interestingly the somatic mutations in position 12 (G12), 13 (G13) and 61 (Q61) are found in human cancer cells which mostly affect the intrinsic and GAP-activated GTP hydrolysis, and thus, render them in their GTP-bound forms and hyperactivity (Fig. 2). When Q61 substituted by any other amino acid the nucleophilic attack on the γ-phosphate is impaired and the enzyme function is impaired, too (Buhrman, Kumar, Cirit, Haugh, & Mattos, 2010) (Scheidig, Burmester, & Goody, 1999) (Scheffzek, et al., 1997). Furthermore, oncogenic mutations leading to the substitution of G12 or G13 impede the creation of van der Waals bonds between the RAS protein and the related GAP (Scheffzek, et al., 1997). Mutations at G12 or G13 are mostly found in KRAS and HRAS, whereas mutations concerning Q61 are commonly found in NRAS (Pylayeva-Gupta, et al., 2011) .

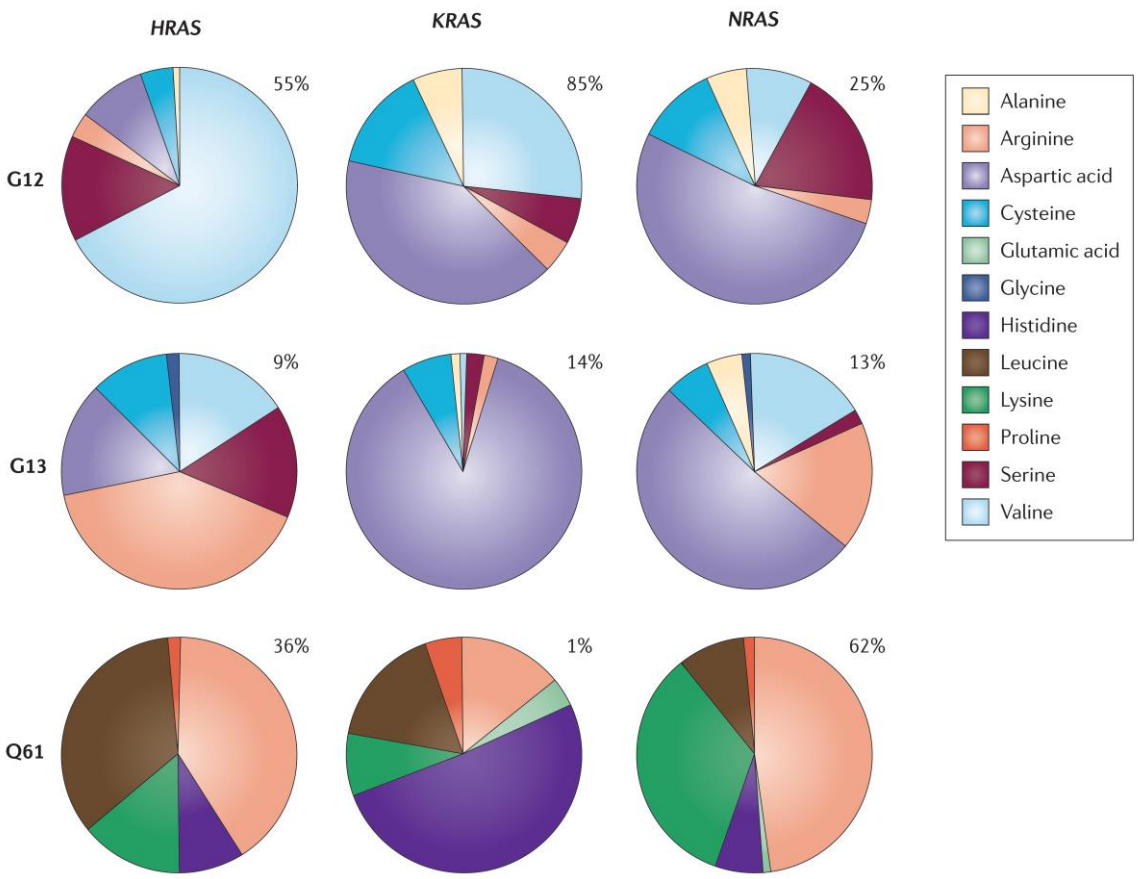

Figure 2: Frequency of the mutations at G12, G13 and Q61 found in the RAS isoforms, HRAS, KRAS and NRAS.
The frequency of mutational substitution at the three positions G12, G13 and Q61 by using pie charts is depicted (Pylayeva-Gupta, et al., 2011). The percentage illustrates the frequency which the given residues are mutated in the within the RAS isoforms HRAS, KRAS and NRAS. Primary data base is the COSMIC database (Pylayeva-Gupta, et al., 2011).

1.5 ERAS, a novel member of the RAS subfamily

Hallmarks of ERAS

Embryonic stem cell-expressed RAS (ERAS) shares with all of the other RAS proteins the highly-conserved G domain with 5 conserved motifs G1-G5 (Fig. 3). However, ERAS shows a critical amino acid deviation in the G1 motif: The glycine 50 (G12 in HRAS) is replaced by a serine (S50), which consequently makes ERAS GAP insensitive and therefore hyperactive (Nakhaei-Rad, et al., 2015); it binds tightly to GTP but does not properly hydrolyze it. The deviation of G12 is already known in connection with somatic mutations of RAS proteins and correlated with cancer development (Bos, 1989; Pylayeva-Gupta, et al., 2011). The G2 and G3 motifs (effector binding site) of RAS proteins are recognized with RAS-binding domain (RBD) or RAS association domain of effector proteins. Notably, in comparison with other RAS proteins, ERAS harbors different amino acids sequence in its

effector binding site family (Fig. 3), which leads to a different effector-selectivity compared with the other RAS proteins. In addition, ERAS contains a specific, 38-amino acid-long, extended N-terminus, taking a role in the ERAS signaling-activity (Nakhaei-Rad, et al., 2015).

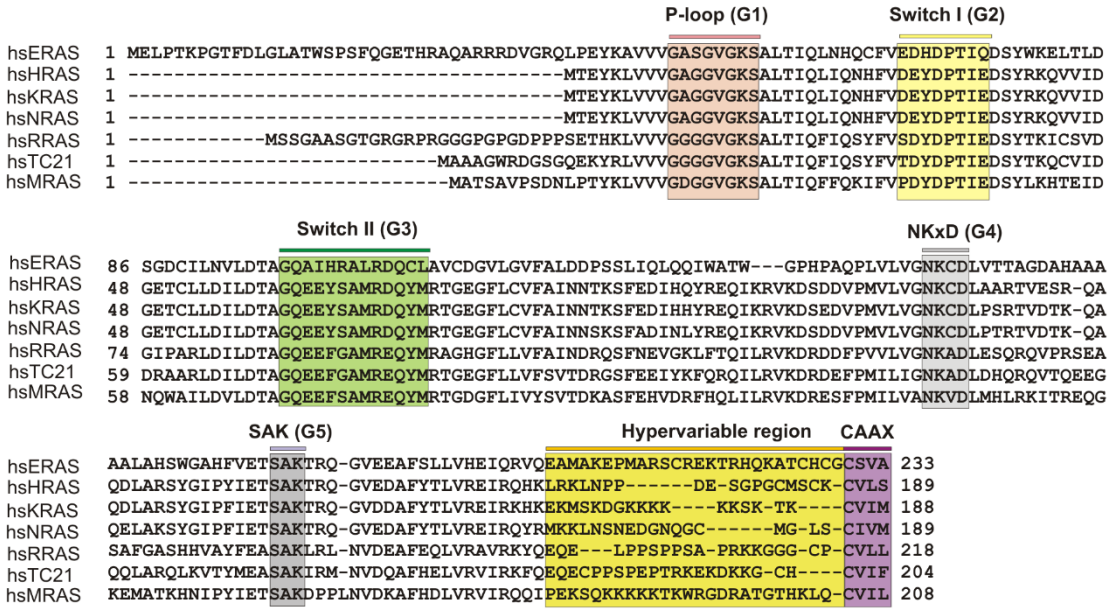

Figure 3: Alignment of hsRAS isoforms, such as ERAS, HRAS, KRAS, NRAS, RRAS, TC21 and MRAS.
An alignment of different RAS proteins is shown. Well visible is the extended N-terminus *hs*ERAS harbors.

Expression of ERAS

In 2003, ERAS was described for the first time by the group of Yamanaka. They reported that this newly discovered protein is specifically expressed in undifferentiated mouse embryonic stem cells. They introduced ERAS to harbor properties being important for the maintenance of the tumor-like abilities of these cells (Takahashi, Mitsui, & Yamanaka, 2003). More recently, the expression of ERAS at the mRNA level was also detected in different entities of human cancer cell lines, including colorectal (HCT-116, DLD-1, LS174T and HT-29), pancreatic (RWP-1 and MIAPaCa-2), and breast carcinoma (AMB-231) cells. However, normal cell lines did not express ERAS at the mRNA level (NF24, NF25, NF26, mesothelial cells and lymphocytes) (Yasuda, Yashiro, Sawada, Ohira, & Hirakawa, 2007). In 2010, ERAS was then, not only at the mRNA level, but also at the protein level, detected in gastric cancer cell lines (e.g. GCIY, NUGC-4 and MKN-74)

(Kubota et al., 2010). In further studies, it was reported that about 44% of gastric cancer tissues express ERAS which significantly correlated with invasion depth, histological type, clinical stage and curability. In addition, patients with ERAS-negative tissue had a significant poorer prognosis than patients with ERAS-positive tissue (Kaizaki et al., 2009). Also, ERAS expression was found in several neuroblastoma cell lines (e.g. SH-SY5Y and IMR-32). It has been suggested that ERAS expression promotes the transforming activity and the resistance to tested chemotherapeutic agents in these cells (Aoyama, 2010).

Expression of ERAS in normal cell-After ERAS expression was firstly described in embryonic stem cells of mice and then in different human carcinoma cell lines, ERAS was recently reported in quiescent Hepatic Stellate Cells (qHSC) (Nakhaei-Rad, et al., 2016). HSCs are liver-resident mesenchymal stem cells, playing an important role in regeneration and fibrosis of the liver (Yin, Evason, Asahina, & Stainier, 2013). After injury of the liver, HSCs get activated and ERAS expression is downregulated (Nakhaei-Rad, et al., 2016). The HSCs then exhibit myofibroblast-like properties and contribute to the production of extracellular matrix, which leads in pathological extent to liver fibrosis (Kordes & Häussinger, 2013). It was shown that ERas is specifically expressed in qHSCs of *Rattus norveticus* and takes a key role within the signaling cascades controlling the maintenance of the stem cell properties of HSCs. ERAS may regulate effectors such as RASSF5/Hippo and PI3K α/δ, LATS kinase and AKT. Their activation may lead to inhibition of proliferation and induce the survival of the cells. ERAS, thus, is indispensable for HSCs to remain in their quiescent state. Furthermore, it was shown that once HSCs get activated during liver injury, expression of ERAS gets downregulated and the already described signaling pathways fail to appear. Moreover, common RAS proteins are expressed in activated HSCs (aHSC), leading to an activation of the MAPK pathway resulting in differentiation of the cells (Nakhaei-Rad, et al., 2016).

ERAS and somatic cell reprogramming- Since 1998 pluripotent embryonic stem cells were generated from human blastocysts in order to find a new therapeutic option to treat patients with degenerative diseases (Thomson et al., 1998). Beyond its expression in undifferentiated embryonic stem cells of mice, cancer cells, and hepatic tissue, ERAS gene was classified as one out of 20 embryonic stem-cell (ES cell) specific genes, so called ES cell-associated transcripts (ECATs) (Takahashi, Murakami, & Yamanaka, 2005). It was shown that ERAS is a crucial factor for the generation of induced pluripotent stem cells (iPSCs) (Takahashi &

Yamanaka, 2006). However, injection of ES cells was consequently followed by formation of teratoma. Though, ERAS deficient ES cells formed smaller teratoma when injected subcutaneously. Furthermore, ERAS deficient ES cells showed a lower proliferation rate than wildtype ES cells. Induced re-expression of ERAS or forced expression of PI3K led to a phenotype of wildtype ES cells (Takahashi, et al., 2005). The group of Takahashi concluded in 2005 that ERAS is not essential, but promotes ES cell proliferation. In addition, ERAS was described as important facilitator of somatic cell reprogramming by activating AKT which yields the inhibition of the transcription factor FoxO1 being a barrier to the induction of iPSCs. Connected to this, a common basis of somatic cell reprogramming and cancer initiation was suggested (Yu et al., 2014).

Aim of this doctoral thesis

The members of the RAS protein family take crucial roles in intracellular cell signaling due to their properties as GTPases. The described biological functions show that these proteins are involved in cell processes like proliferation, differentiation and apoptosis. This knowledge suggests that RAS proteins take part in the process of carcinogenesis, which is already known for several RAS proteins such as KRAS. However, the youngest RAS family member, ERAS and its functions especially in tumors, have been unknown so far. Previous works about ERAS indicate that this protein harbors functions being important for the tumor-like properties of embryonic stem cells, suggesting that being part of the carcinogenesis, ERAS might be an interesting new target for targeted chemo-therapy. The main objective of this work is, thus, to analyze the expression of ERAS in several human cancer-entities by using established cancer cell lines. However, a validated system has not commonly been known so far. Thus, this work firstly aimes at establishing validated tools for the mainly intended expression analyses.

Therefore, several sets of primers were designed and then validated. Secondly, a specific anti-ERAS antibody was validated, too.

The objective of the present work is to analyze the expression of ERAS at the mRNA level by conducting qPCR analysis. In the next step, ERAS protein function in Tumor cells are to be investigated by perfoming Western blot analysis and Pull-down assay.

Chapter 2

Materials:

2.1 Chemicals and reagents

Table 2: List of chemicals and reagents

Chemicals and reagents	Manufacturer/ Distributor	Storage
β-Glycerolphosphate	SIGMA Life Science	4°C
β-Mercaptoethanol	SIGMA Life Science	4°C
Acrylamide	Sigma Aldrich, München	RT
Agarose	Sigma Aldrich, München	RT
Amersham ECL Prime Western blotting Detection Reagent	GE Healthcare Life Science	4°C
Ammonium persulfate (APS)	Sigma Aldrich, München	-20°C
Ampicillin	Sigma Aldrich, München	RT
Bradford Reagent	BIO-RAD, München	4°C
Bromophenol blue	Roth, Karlsruhe	4°C
Chloramphenicol	Sigma Aldrich, München	-20°C
Coomassie brilliant blue, R250	Roth, Karlsruhe	RT
ddH_2O	Merck, Darmstadt	RT
Deoxynucleoside triphosphate	Qiagen, Hilden	-20°C
Dimethyl sulfoxide (DMSO)	Sigma Aldrich, München	RT
Dithiothreitol (DTT)	GERBU Biotechnik, Wieblingen	4°C
Dulbeccos´s Modified Eagle Medium 1x (DMEM)	Gibco™, Darmstadt	4°C
EDTA-free protease inhibitor	Roche Applied Science, Penzberg	4°C
Ethanol	Roth, Karlsruhe	RT
Ethidium bromide (EtBr)	AppliChem , Darmstadt	RT
Fetal bovine serum (FBS)	Gibco™ Thermo Fisher Scientific	-20°C
GeneRulerTM DNA Ladder Mix	Thermo Fisher Scientific	4°C
Glycerol	Roth, Karlsruhe	RT
Hydrochloric acid HCL	Roth, Karlsruhe	RT

Horse Serum (PAN Biotech, P30-0701)	Sigma-Aldrich	-20°C
Igepal (NP40)	MERCK Chemicals, Darmstadt	RT
Isopropyl β-D-1-thiogalactopyranoside (IPTG)	GERBU Biotechnik, Wieblingen	4°C
LB-Agar-Powder	AppliChem	RT
Magnesium chloride	Sigma Aldrich, München	RT
McCoy's 5a medium modified	Gibco™, Darmstadt	4°C
Methanol	Roth, Karlsruhe	RT
Milk powder	Roth, Karlsruhe	RT
PageRuler ™ Prestained Protein Ladder	Thermo Fisher Scientific	4°C
Phosphate-buffered saline (PBS)	PAN Biotech	RT
Penicillin/Streptomycin (P/S)	Genaxxon Bioscience, Ulm	-20°C
Roswell Park Memorial Institute medium (RMI-1640)	Gibco™, Darmstadt	4°C
Potassium chloride	MERCK Chemicals, Darmstadt	RT
Sodium chloride	Sigma Aldrich, München	RT
Sodium dodecyl sulfate (SDS)-Pellets	Roth, Karlsruhe	RT
Sodium orthovanadate (Na3VO4)	SIGMA Life Science	-20°C
SYBR Green	Thermo Fisher Scientific	-20°C
Tetramethylethylenediamine (TEMED)	AppliChem, Darmstadt	4°C
Trishydroxymethylaminomethane (Tris)	Roth, Karlsruhe	RT
Trypan blue	BIO-RAD, München	RT
TurboFect Transfection Reagent	Thermo Fisher Scientific	4°C
Tween-20	Sigma Aldrich, München	RT

2.2 Instruments and Equipment

Table 3: List of instruments and equipment

Name of instrument	Manufacturer
7500 Real Time PCR System	Applied Biosystems
Agarose Gel Electrophoresis equipment	BIO-RAD
BioPhotometer Plus	Eppendorf
Centrifuge 5415D	Eppendorf
Centrifuge 5417R	Eppendorf
Centrifuge Hettich universal 30 PF	Hettich
ECL Chemocam Imager	Intas
Freezer HERA freeze	Thermofisher
Incubator HERA cell 150	Heraeus
Labfuge 400R	Heraeus
Light microscope Primovert 28	Zeiss
Mastercycler	Eppendorf
Peqlab Nano Drop 2000c	Thermo Scientific
SDS-PAGE apparatus	BIO-RAD
Thermo-Shaker	Universal Labortechnik
Sterile bench Hera Safe	Heraeus
TC 20 Automated Cell Counter	BIO-RAD
Vortexer: VF 2	IKA Labortechnik

2.3 Antibodies

Table 4: List of primary antibodies

Antibody	Manufacturer
Anti-hsERAS, IgG (goat)	Santa Cruz Biotechnology (sc-51077)
Anti-FLAG , IgG (mouse)	Sigma (F7425)
Anti-GAPDH, IgG (rabbit)	Cell signaling (2118 S)
Anti- γTubulin, IgG (mouse)	SIGMA Life Science (T6557)

Table 5: List of secondary antibodies

Antibody	Manufacturer
Anti-goat HRP-linked IgG	Thermo Fisher Scientific
Anti-Mouse HRP-linked IgG	Dako (P0161)
Anti-Rabbit HRP-linked IgG	Cell signaling (7074S)

2.4 Enzymes

Table 6: List of enzymes

Enzyme	Manufacturer
BamH I (restriction enzyme)	Thermo Fisher Scientific
DNase	Ambion
FAST AP (thermosensitive alkaline phosphatase)	Thermo Fisher Scientific
MMLV (reverse transcriptase)	Promega
Phusion Hot Start II High-Fidelity DNA Polymerase	Thermo Fisher Scientific
Rnasin	Ambion
T4 ligase	Thermo Fisher Scientific
Trypsin	Genaxxon Bioscience, Ulm
Xho I (restriction enzyme)	Thermo Fisher Scientific

2.5 Kits

Table 7: List of used Kits

Kit	Manufacturer
Ambion RNA	Life technologies
cDNA synthesis Kit	Promega
NucleoBond® Xtra Midi / Maxi	Macherey-Nagel
RNeasy Plus Mini Kit	QIAGEN
Qiaquick Gel extraction Kit	QIAGEN
Qiaquick PCR Purification Kit	QIAGEN
Qiaprep Spin Miniprep Kit	QIAGEN

2.6 Other Materials

Table 8: List of other materials

Material	Manufacturer
25cm² Flasks	TPP
75cm² Flasks	TPP
150cm² Flasks	TPP
100 tissue culture dishes	TPP
6 well-plates	Falcon™
15ml Falcon tubes	Falcon™
50ml Falcon tubes	Falcon™

Amersham Protran Nitrocellulose Blotting Membranes	GE Healthcare Life Sciences
MicroAmp® Optical 96-Well Reaction Plate	Applied Biosystems
Counting slides	BIO-RAD
Filter paper Western blot	Whatman

2.7 Oligonucleotides

Table 9: List of oligonucleotides

Description	**Oligonucleotide (sequence 5'→3')**	**Intended use**
hsERAS 3 fw	CGCTGACCATCCAGCTGAAC (20)	RT-PCR
hsERAS 3 rv	CCACTGTCCAGGGTCAACTC (20)	RT-PCR
hsERAS 1 fw	CAACAAAGCCTGGCACCTTC (20)	RT-PCR
hsERAS1 rv	ACCACCACAGCCTTGTACTC (20)	RT-PCR
hsERAS 2 fw	CACGGACACAGAGCCTGC (18)	RT-PCR
hsERAS 2 rv	GTTTCCCCCTGGAAGGAAGG (20)	RT-PCR
hsGAPDH fw	GGAAGGTGAAGGTCGGAGTCA (21)	RT-PCR
hsGAPDH rv	GTCATTGATGGCAACAATATCCACT (25)	RT-PCR
hsMRAS fw (BamHI)	CGCGGATCCATGGCAACCAGC GCCGTCCCCAGT (33)	PCR
hsMRAS rv (XhoI)	CCGCTCGAGTTAAAGATCACA CATTGCAGTTTG (33)	PCR
TBP fw	ACAACAGCCTGCCACCTTA (19)	RT-PCR
TBP rv	GAATAGGCTGTGGGGTCAGT (20)	RT-PCR
SDHA fw	GCCAGGACCTAGAGTTTGTTCA (22)	RT-PCR
SDHA rv	CTTTCGCCTTGACTGTTAATGA (22)	RT-PCR

2.8 Plasmids

Table 10: List of vector and plasmids

Plasmid	Description	Selection marker	Manufacturer
pcDNA 3.1	Mammalian expression	amp	OriGene
pGFP-C-shLenti	Mammalian expression	chlor	OriGene

Figure 4: pGFP-C-shLenti vector

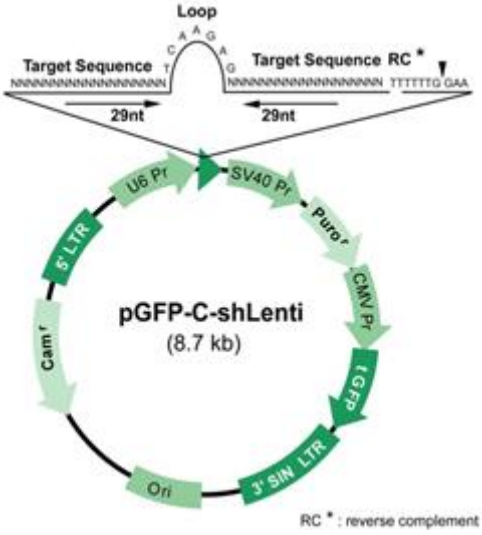

Figure 4: pGFP-C-shLenti vector
U6 promoter (U6 Pr): expression of the shRNA**; SV40 promoter (SV40 Pr):** expression of the puromycin **(Puro^r)** resistant gene; **CMV promoter (CMV Pr):** expression of **tGFP**; Chloramphenicol **(Cam ^{r}):** bacterial selection marker.

2.9 Buffers and solutions

Table 11: List of buffers and solutions (name composition and storage)

Buffer	Composition	Storage
APS	5 g APS 50 ml ddH_2O	-20°C
Blocking solution	TBS-T/N buffer	4°C

	5% milk powder	
Fish-buffer	50 mM Tris/HCL	-20°C
	100 mM NaCl	
	2 mM MgCl2	
	1 % IGEPAL CA-630	
	10 % Glycerol	
	20 mM ß-Glycerolphosphate	
	1 mM ortho Na3VO4	
	1 tablet of protease inhibitor	
IPTG	2.83 g IPTG	-20°C
	ad 10 ml ddH2O	
5x Laemmli buffer	250 mM Tris/HCl	-20°C
Use 1:5	50 % Glycerol	
	10 % ß-Mercaptoethanol	
	10 % SDS	
	0.25 % Bromophenol blue	
PBS	10 % (v/v) DPBS	RT
	Sterile ddH2O	
SDS destaining solution	20 % (v/v) Methanol	RT
	10 % (v/v) Acetic acid	

SDS-PAGE resolving buffer (pH 8.8)	750 mM Tris/HCl 0.2 % (v/v) SDS	RT
10x SDS-PAGE running buffer Use 1:10	250 mM Tris/HCl 1.92 M Glycerol 1 % (v/v) SDS	RT
SDS-PAGE stacking buffer (ph 6.8)	250 mM Tris/HCl 0.2 % (v/v) SDS	RT
SDS staining solution	40 % (v/v) Methanol 10 % (v/v) Acetic acid 4 g/l Coomassie brilliant blue R250	RT
FPLC Standard buffer	30mM Tris pH 7.5 100 mM NaCl 3mM DTT 5mM $MgCl_2$	4°C
50x TAE buffer (pH 8.5) Use 1:50	2 M Tris/HCl 50 mM EDTA	RT
10x TBS Use 1:10	25 mM Tris/HCl 150 mM NaCl 3 mM KCl	RT

TBS-N	TBS 0.05% NP40	RT
TBS-T	TBS 0.05% Tween	RT
10x Transfer buffer Use 1:10	25 mM Tris 192 mM Glycin 10% Methanol 0.02% SDS	RT
1x Transfer buffer		4°C
1xTrypsin/EDTA (0.5%/0.2%)		4°C

2.10 Cell lines

Table 12: List of cell lines

Cell line	Description	Species	Origin
CAPAN-1 (Medium 1)	Pancreatic ductal adenocarcinoma	Human	Department of General, Visceral and Pediatric Surgery (Düsseldorf)
CAPAN-2 (Medium 2)	Pancreatic ductal adenocarcinoma	Human	Department of General, Visceral and Pediatric Surgery (Düsseldorf)
DLD-1 (Medium 3)	Colorectal adenocarcinoma	Human	Department of General, Visceral and Pediatric Surgery

			(Düsseldorf)
HCT-116 (Medium 4)	Colorectal adenocarcinoma	Human	Department of General, Visceral and Pediatric Surgery (Düsseldorf)
HT-29 (Medium 4)	Colorectal adenocarcinoma	Human	Department of General, Visceral and Pediatric Surgery (Düsseldorf)
LOVO (Medium 3)	Colorectal adenocarcinoma	Human	Department of General, Visceral and Pediatric Surgery (Düsseldorf)
MIAPaCa-2 (Medium 6)	Pancreatic ductal carcinoma	Human	Department of General, Visceral and Pediatric Surgery (Düsseldorf)
SW480 (Medium 3)	Colorectal adenocarcinoma	Human	Department of General, Visceral and Pediatric Surgery (Düsseldorf)
HEK (Medium 7)	Human embryonic kidney cells	Human	Institute of Biochemistry and Molecular Biology II (Düsseldorf)
SH-SY5Y (Medium 8)	Neuroblastoma cells	Human	Department of Neuropathology (Düsseldorf)
IMR-32 (Medium 7)	Neuroblastoma cells	Human	Department of Neuropathology (Düsseldorf)
BPH-1 (Medium 3)	Benign prostate hyperplasia cells	Human	Department of Urology (Düsseldorf)
PNT-2 (Medium 3)	Normal prostate epithelia cells immortalized with SV40	Human	Department of Urology (Düsseldorf)

NCCIT (Medium 3)	Placenta cancer cells	Human	Department (Düsseldorf)	of Urology
Tera-1 (Medium 4)	Teratocarcinoma cells	Human	Department (Düsseldorf)	of Urology
Tera-2 (Medium 4)	Teratocarcinoma cells	Human	Department (Düsseldorf)	of Urology
NT-2 (Medium 4)	Teratocarcinoma cells	Human	Department (Düsseldorf)	of Urology

Chapter 3 Methods:

3.1 Cell culture

3.1.1 Tumor cell lines and culturing conditions

The cell lines DLD-1, LOVO and SW480 were cultured in RPMI 1640 medium (Roswell Park Memorial Institute medium) supplemented with 10% fetal bovine serum (FBS) and 1% Penicillin/Streptomycin. The cell lines HCT-116 and HT-29 were fed with McCoy's 5a medium supplemented with 10% FBS. The cell line CAPAN-1 was cultured in RPMI medium supplemented with 20% FBS, the cell line CAPAN-2 was cultured in RPM medium supplemented with 15% FBS. The cell line MIAPaCa-2 was cultured in DMEM medium (Dulbecco's Modified Eagle's Medium) supplemented with 20% FBS and 2.5% Horse serum. The cell line HEK was cultured in DMEM medium supplemented with 10% FBS. All cell lines were incubated at 37 °C under an atmosphere of 5 % CO2.

Table 13: List of cell line specific media

Name of medium	Ingredients
Medium 1	RMI-1640 + 20% FBS +

	1% Penicillin/Streptomycin
Medium 2	RMI-1640 + 15% FBS + 1% Penicillin/Streptomycin
Medium 3	RMI-1640 + 10% FBS + 1% Penicillin/Streptomycin
Medium 4	McCoy's 5a medium modified + 10% FBS + 1% Penicillin/Streptomycin
Medium 6	DMEM (PAN Biotech,P04-03590) + 20% FBS + 2.5% Horse Serum (PAN Biotech, P30-0701) + 1% Penicillin/Streptomycin
Medium 7	DMEM (PAN Biotech,P04-03590) + 10% FBS + 1% Penicillin/Streptomycin

3.1.2 Cell passaging

When the cells were confluent the medium was removed and the cells were washed with PBS -/- (without magnesium and without calcium). Afterwards the PBS was removed and to detach the cells 1.5 mL of trypsin was added. Then the cells were incubated for 10/15 minutes (until the cells were detached). To deactivate the trypsin, 8.5 mL of medium containing FBS was added, and the whole suspension was homogenized throughout pipetting a few times. The cells and the solution were transferred to a 15 mL Falcon tube and centrifuged for 5 min with a speed of 1200 rpm at room temperature (RT) to remove the rest of trypsin and dead cells. The supernatant was then removed and the cells were resuspended in 3 mL of the destined medium (see table 12). Then according to the growth rate of the cell lines, they were passaged 1 to 5 and transferred to a 75 cm^2 Flask with fresh medium and incubated until they were confluent again.

3.1.3 Cell count measurement with TC20TM Automated Cell Counter

Optional: The cells were counted by the TC 20 Automated Cell Counter to prepare certain experiments. Therefore 10 µl of the cells were added to 10 µl of Trypan blue and put on a counting slide which was placed in the cell counter. For the RNA isolation $5x10^5$ cells were seeded on one well of a 6-well plate. The cells were then cultured in 2 mL of the destined medium (see table 12) until they were confluent. To analyze the expression of ERAS at the

protein level $8x10^5$ cells were seeded on a 10cm dish and cultured in 5 mL of the destined medium (see table 12) until they were confluent.

3.1.4 Cryopreservation of the cells

To freeze the cells, the medium was removed and the cells were washed with 10 mL PBS -/- . Then 1.5 mL trypsin was added and the cells were incubated for 10 minutes. The trypsin was then deactivated by adding 8.5 mL of medium containing FBS. Following the suspension was transferred to a 15 mL Falcon tube and centrifuged with a speed of 1200 rpm for 4 minutes at RT. The supernatant was removed and the cells were resuspended in 3 mL of the destined medium (see table 1). 2 million of the dissolved cells were then added to 600 µl of the freezing medium (see table 2 below) in a cryotube and stored at -80°C .

For defrosting, the cells in the cryotube were melted at 37°C and quickly added to 5 mL of the warm destined medium in a 15 mL Falcon tube. The solution was centrifuged for 4 minutes with a speed of 1200 rpm at RT. Afterwards the supernatant was removed and the cells were resuspended in 3 mL of the destined medium, transferred to a 75 cm² Flask and incubated at 37°C .

Table 14: Freezing medium

Components	Amount	Total
DMSO 10 %	60 µl	
FBS 10 %	60 µl	600 µl
Destined medium 80 %	480 µl	

3.2 RNA Techniques

3.2.1 RNA Isolation

To isolate the RNAs the cells were first seeded on 6 - wells and incubated until they were confluent. Following the medium was removed and the cells were washed with PBS -/-. The cells were then directly lysed by using 600 µl of RLT buffer Plus (supplied in the RNeasy Plus Mini Kit) and transferred to a 1.5 mL tube. (The lysed cells were stored at -80°C until use)

The isolation of the RNAs was done by using the QIAGEN RNeasy Mini Kit. Following the concentration of the RNA was measured by the Peqlab Nano Drop 2000c.

3.2.2 DNase Treatment

To make sure that the RNA samples do not contain any genomic DNA, they were treated with DNase. Depending on the concentration of the RNAs 3 to 4,5 µg of these were used and the volume was filled up to 32 µl with double destilled (dd) water. Subsequent 4 µl of the buffer, 1 µl of the DNase and 1 µl of the RNase inhibitor were added. The samples were then incubated at 37 °C for 30 minutes. Following 5 µl of the inactivation reagent was pipetted to the samples and then the samples were incubated for 2-5 minutes at RT. The samples were now centrifuged for 1.5 minutes at 4 °C (10.000 rcf). The supernatant has to be saved.

3.2.3 cDNA synthesis

To synthesize the cDNA, 1 µg of the RNA and 1 µl of oligo dTs were mixed. The volume was filled up to 10 µl with dd water. The solution was incubated first at 70 °C for 5 minutes, then on ice for 5 minutes. Following 10 µl of the Master Mix were added to the samples. The samples were now placed in the Mastercycler. The following program was used:

Table 15: cDNA synthesis PCR program

Temperature (°C)	Time (min)
25	10 minutes
42	1 hour
70	15 minutes
4	Hold

The synthesized cDNA was diluted 1:5 and stored at -20 °C until use.

3.2.4 Reverse Transcription (RT) – PCR

To analyze the expression of ERAS at the mRNA level, the synthesized cDNAs were used for a quantitative PCR. This PCR was done by using SYBR Green. Therefore 5 µl of the diluted (1:5) cDNA samples were added to 15 µl of the Master Mix. For each sample duplicates were prepared.

The following program was used:

Table 16: RT-PCR program

Temperature	Time (min)	Cycle
95 °C	10 minutes	
60°C	15 seconds	x 40
60 °C	1 minute	

Table 17: RT-PCR Master Mix

Reagents	Amount
SYBR GREEN	10 µl (2x)
FW primer	1 µl (10 µM)
RV primer	1 µl (10 µM)
cDNA	5 µl / 2 µl (TBP Master Mix)
ddH_2O	3 µl / 6 µl (TBP Master Mix)
	Σ= 20 µl

To determine the relative amount of mRNAs the average of the CT-values was calculated and then standardized on the internal control TBP (ΔCT). To compare the data to each other the ΔCT-values were standardized on the ΔCT-value of one of the samples (ΔΔCT) and then the data were represented graphically ($2^{-\Delta CT}$; $2^{-\Delta\Delta CT}$).

After the RT-PCR program finished, the samples were loaded on a 2% agarose gel to visualize the amplified cDNA and to prove the absence of primer dimers.

3.3 DNA Techniques

3.3.1 Cloning

In order to validate the anti-ERAS antibody, a Blot with transfected RAS constructs was made. Therefore, the required RAS constructs were generated by cloning. Firstly, for each construct a 0.2 mL tube was labeled and placed on ice. Then 1 µl of the template was added to the Master Mix (see Table 17). The samples were then placed on the Mastercycler and following program was used.

Table 18: Components of PCR

Component	Amount
Construct plasmid	1 µl
Buffer	20 µl
dNTPs	2 µl
Primer fw	1 µl
Primer rv	1 µl
Phusion Hot Start II High-Fidelity DNA Polymerase	1 µl
dd H_2O	74 µl
	Σ = 100 µl

Table 19: PCR program

Temperature	Time	Cycle
98 °C	1 min	
98 °C	45 sec	
51-73 °C	45 sec	x35
72 °C	45 sec	
72 °C	10 min	
4°C	hold	

Analytical Agarose Gel Electrophoresis

After amplification, the PCR construct was mixed with loading dye and then loaded on a 1 % agarose gel. For the electrophoresis Tris-Acetate-EDTA buffer (TAE buffer) was used. The electrophoresis was then run at 100 V for 30 min. As a size marker GeneRulerTM DNA Ladder Mix (Thermo Fisher Scientific) was used. The gel was analyzed by using UV-light.

Gel extraction

After analysis of the agarose gel, the amplicons were cut out and weighed. Following gel extraction was done by using the Gel Extraction Kit by Quiagen. DNA was eluted in 20 µl of dd H_2O.

Digestion with BamH I and Xho I

To insert the plasmid of the construct to a vector (pcDNA 3.1), vector and construct were cut by the restriction enzymes BamH I and Xho I. The following components were accordingly mixed and incubated for 1 h and 30 min at 37 °C.

Table 20: Master mix for Digestion I

Component	Insert	Vector
DNA	20 µl	10 µl
dd H_2O	6 µl	16 µl
Buffer	3 µl	3 µl
Enzyme	1.5 µl	1.5 µl
	Σ= 30.5 µl	Σ= 30.5 µl

After the first digestion, the samples were purified according to the PCR purification Kit (Quiagen) and eluted with 30 µl of dd H_2O. Subsequently the vector and the insert were digested with the other restriction enzyme:

Table 21: Master mix for Digestion II

Component	Amount
DNA	26 µl
Buffer	3 µl
Enzyme	1.5 µl
	Σ= 30.5 µl

Later, PCR purification was repeated. The DNA was again eluted with 30 µl of dd H_2O.

Dephosphorylation of the vector

Dephosphorylation of the vector was done after the digestion with the second restriction enzyme. To dephosphorylate the vector a thermosensitive alkaline phosphatase (FAST AP) was used. DNA, the enzyme and its specific buffer were mixed as follows:

Table 22: Master mix for Dephosphorylation

Component	Amount
DNA of the vector	26 µl
Buffer 10x	3 µl
FAST AP	1.5 µl
	Σ = 30.5 µl

After Dephosphorylation was done, PCR purification was performed. The DNA was eluted with 30 µl of dd H_2O.

Ligation

After insert and vector were cut and the vector was dephosphorylated, ligation of both samples followed. Therefore, a Master mix was prepared (see Table 22). The tube containing the Master mix was incubated for 2h at RT. Following Deactivation of the T4 Ligase was done by heating the sample at 72 °C for 5 min.

Succeeding, transformation of the construct was done (See section 3.3.3).

Table 23: Master mix for Ligation

Component	Amount
Target DNA	10 µl
Vector DNA	2 µl
Buffer	2 µl
T4 Ligase	1.5 µl
dd H_2O	11.5 µl
	Σ = 27 µl

3.3.2 Transfection

The transient transfection of HEK cells was done with TurboFect Transfection Reagent. TurboFect is a polymer that forms positively-charged complexes with DNA which are compact and stable. This leads to a protection of the DNA molecules from degradation and therefore a more facile delivery of the DNA into the cells.

$4x10^5$ HEK cells were seeded on 6 wells of a 6 well plate and cultured with 2mL DMEM supplemented with 10% FBS and 1% Penicillin/Streptomycin for 48 hours. Then 2-3 µg of the target DNA was added to 200 µl of DMEM-/- (without FBS and without antibiotics) and mixed with 4 µl of TurboFect. The samples were vortexed and then incubated for 20 min at RT. Following the mixture was added to the 6 wells and incubated. After 6 hours the medium was changed and the cells were cultured until lysis.

3.3.3 Transformation

To amplify and store the plasmids, transformation was performed. For this purpose, 1 to 2 µl of the target plasmid were added to 30 µl of chemical competent *E. coli* of the strain XL1-blue. The bacteria were then incubated for 30 min on ice, and after that for 90 sec heated at 45 °C . Subsequently the tube was placed on ice. Afterwards 1 mL of warm SOC medium was immediately added, and the bacteria were cultured for 1h and 30 min at 37 °C in a shaker (140 rpm). After incubation, the cells were centrifuged at 5000 rpm for 5 min. The supernatant was removed and thereafter the bacteria were resuspended in 100 µl of warm LB medium. The suspension was then distributed on a pre-warmed LB-plate containing the destined selection marker e.g. ampicillin. For growth of bacterial colonies, the plates were placed in an incubator (37 °C) overnight.

3.3.4 DNA isolation from E. coli

Mini-preparation

For generating low amounts of the target plasmid one single bacterial colony (after transformation) was transferred to 5 mL of LB-medium containing the destined selection marker (1:1000) and cultured at 37 °C on a shaker (140rpm) overnight. Subsequently the target plasmid was isolated by using the Quiaprep Spin Miniprep Kit and the DNA was eluted was with 30µl of dd H_2O. The DNA concentration was determined by using the Peqlab Nano Drop 2000c.

Midi-preparation

For generating larger amounts of the target plasmid, a sterile pipette tip was used to scratch the bacteria from the frozen surface of the destined glycerol stock (see Preparation of glycerol stocks) and put into 5 mL of warm LB medium containing the required selection marker (1:1000). Afterwards the bacteria were pre-cultured at 37°C on a shaker (140rpm) overnight. Afterwards the pre-culture was added to 500 mL of warm LB-medium and an overnight culture at 37°C on a shaker followed. The isolation of the target plasmid was then performed by using the NucleoBond® Xtra Midi / Maxi by Macherey-Nagel, and eluted in 100 µl of dd H_2O. The DNA concentration was determined by using the Peqlab Nano Drop 2000c.

Generating Glycerol stocks

To store the bacteria containing the plasmid, 750 µl of the culture (Midi-preparation) were added to a cryotube and then mixed with 250 µl of 80 % glycerol. After that the tube was snap frozen in liquid nitrogen. The stock was stored at -80°C.

3.3.5 Determination of the nucleic acid concentrations

The concentration of nucleic acids was determined by using the Peqlab Nano Drop 2000c. Therefore, the spectrometer was blanked with the elution buffer before adding 1 µl of the sample. Nucleic acids have an absorbance maximum at a wavelength of 260 nm, proteins at 280 nm. The calculated ratio of these absorbances (A260/A280) is used to evaluate the purity of the sample.

3.4 Protein Techniques

3.4.1 Generating total cell lysates

For generation of total cell lysates, cells were cultured on a 10cm plate until they were confluent. Subsequently the medium was removed and the cells were washed with 5 mL of PBS -/-. The washing buffer was removed and 1 mL of fresh PBS -/- were added to the plate. The cells were then scratched down and transferred to an Eppendorf tube. Following the cell suspension was centrifuged at 12000 rpm for 5 min at 4°C . The supernatant was removed and the dry cell pellet was kept at -80°C until use.

For lysis the cells were resuspended in 250 µl of following lysis buffer:

Table 24: Fish buffer

Component	Concentration
Tris/HCl pH 7.4	50 mM
NaCl	100 mM
MgCl2	2 mM
Igepal Ca-630	1 %
Glycerol	10 %
β -Glyceolphosphate	20 mM
Ortho Na3VO4	1 mM
Protease inhibitor	1 tablet

After lysis the suspension was centrifuged for 5 min at 12000 rpm at 4 °C . Then the supernatant containing the proteins was transferred to a new tube and placed on ice. The pellet was discarded.

3.4.2 Determination of protein concentrations

In order to measure the protein concentration Bradford-solution and a corresponding calibration curve with BSA samples were prepared. For determination of the protein concentration 500 µl of Bradford-solution were mixed with 2 µl of total cell lysate in a cuvette and incubated for 5 min. By adding proteins, the Bradford-solution is changing its color and the absorbance maximum shifts from 465 nm to 595 nm. The measured absorbance should lie between 0.2 and 1.0.

3.4.3 SDS-Polyacrylamide gel electrophoresis

Based on the ability of proteins to move within an electric field depending on their molecular size, SDS-Polyacrylamide gel electrophoresis was performed to separate the proteins. Therefore, a polyacryalamide gel consisting of a resolving and a stacking part was made (see Table 24). The cell lysates containing the proteins were mixed with 5x Laemmli buffer and cooked for 10 min at 95 °C . Components of the buffer destroyed secondary and tertiary structures as well as disulfide bonds of the proteins. Furthermore, the proteins were negatively charged which assured a migration towards the cathode. For detecting hsERAS

in total cell lysate of cancer cells, at least 75 µg were loaded. For detecting over-expressed proteins 10 µg were loaded. As a size marker PageRuler ™ Prestained Protein Ladder (Thermo Fisher Scentific) was used. The electrophoresis was run in 1x SDS running buffer at 65 V for 3 h and 30 min.

Table 25: Composition of SDS-PAGE gels

Components	Resolving gel 10%	Stacking gel
Resolving buffer (pH 8.8)	3 ml	/
Stacking buffer (pH 6.8)	/	1.5 ml
Acrylamide	2 ml	0.3 ml
H_2O	1 ml	1.25 ml
TEMED	15 µl	10 µl
10 % APS (w/v)	45 µl	20 µl

3.4.4 Western blot

This method was used to transfer the during electrophoresis separated proteins to a nitrocellulose membrane. Therefore, the nitrocellulose membrane was activated by incubating it for 5 min in water. The gel and the activated nitrocellulose membrane were placed one upon the other between several, in Transfer buffer incubated whatman filter papers. The membrane was placed at the anode so that the negatively charged proteins were transferred to the membrane when an electric field was applied. For transferring the proteins to the membrane, the blotting chamber was filled with 1x Transfer buffer. Proteins were transferred at 100 V for 50 min at 4 °C . Afterwards free binding sites of the membrane were blocked by incubating it for 1 h in 10 mL of 5 % milk solution. Following the membrane was incubated in a 5 % milk solution containing the specific primary antibody at 4 °C overnight (for ratios see Table 21). Membrane was then washed three times, each 10 min with TBS-T/N. After washing, the membrane was incubated for 1 h at room temperature in milk solution containing the secondary antibody (ratio: 1:5000). Subsequently the membrane was washed again three times, each 10 min with TBS-T/N. All incubation steps were carried out on a shaker. Analysis of the western blot was performed by using Amersham ECL Prime Western blotting detection reagent (GE Healthcare Life Science). Therefore 500 µl of solution A containing Luminol Enhancer Solution and 500 µl of solution B containing

peroxide solution were mixed and applied onto the membrane. Signals were visualized using the INTas ChemoCam Imager.

Table 26: Composition of Transfer buffer

Component	Concentration
Tris	25 mM
Glycin	192 mM
Methanol	10%
SDS	0.02%
use 1:10	

Table 27: List of primary antibody ratios

Primary antibody	Ratio	Used milk solution
Anti-hsERAS	1: 700	5 % milk TBS-N
Anti-FLAG	1:2000	5 % milk TBS-T
Anti-γTubulin	1:2000	5 % milk TBS-T
Anti-Panras	1:2000	5 % milk TBS-T

Table 28: Composition of TBS-T/N

Component	Concentration
Tris/HCl	25 mM
NaCl	150 mM
KCl	3mM
Use 1:10 and add 0.5 % Tween-20/ NP40	

3.4.5 Protein visualization with Coomassie brilliant blue R-250 staining solution

To visualize proteins separated by SDS-Polyacrylamide gel electrophoresis, staining with Coomassie brilliant blue R-250 was done. The gel was covered with SDS Staining solution

and heated in a microwave until the solution was boiling. After that the gel was incubated for 15-20 min at RT on a shaker. Subsequently the gel was destained using SDS Destaining solution. Therefore, the solution was heated, and an incubation at RT on a shaker followed. The Destaining solution was constantly changed until the gel was completely destained. Finally, a photo from the gel was made.

3.4.6 GST-Pull-down assay

In order to analyze the expression of hsERAS without strong background GST-Pull-down-Assay was performed. Therefore, GSH coupled sepharose beads were incubated with the GST-bait molecule. Consequently the total cell lysate was added and incubated. Thus, the target protein (prey) bound to the bait molecule. This method allows not only the detection of protein protien interaction but also of the target protein (prey) without a strong background of the total cell lysate.

Firstly an E. coli cell lysate, containing the bait molecule was generated. Therefore, E. coli bacteria expressing the bait molecule (PI3K) were pre-cultured (10 mL of LB medium with antibiotic 1:1000) at 37 °C overnight. Then bacteria were inoculated 1:100 (500 mL LB medium with antibiotic 1:1000 + 5 mL of pre-cultured bacteria) and incubated at 37 °C until the OD reached to 07-0.9. After the desired OD was reached, 0.1 mM IPTG was added to induce the protein expression. The bacteria were then incubated for 4 h at 37 °C . Subsequently the cells were centrifuged at 4500 rpm for 10 min. The supernatant was discarded; the pellet was washed and resuspended with 20 mL of FPLC standard buffer (see Table 28). Afterwards the cells were centrifuged again at 4500 rpm for 10 min. The supernatant was discarded, and the pellet was kept on ice. Subsequently the pellet was again resuspended in 20 mL of FPLC standard buffer + EDTA-free protease inhibitor. The solution was transferred to a beaker surrounded by ice. A magnet was placed in the beaker and the cells were lysed by using the sonicator (at 70 % power, 3 pules of 1.5-2 min each time). The lysate was then transferred to tubes and centrifuged at 20000 rpm for 30 min. Closing the supernatant was aliquoted (1 mL), snap frozen in liquid nitrogen, and kept at -80 °C until use.

Table 29: Composition of FPLC standard buffer

Component	Concentration
Tris pH 7.5	30 mM
NaCl	100 mM
DTT	3 mM
$MgCL_2$	5 mM

The GST-Pull-down assay was performed on ice. As negative control GST lysate was prepared. As positive control served purified hsERAS (kindly provided by Hossein Nakhaeizadeh). 500 µl of GSH-beads were washed three times with freshly prepared FISH buffer and each time centrifuged at 500 g for 30 sec. After washing 250 µl of the beads were mixed with 500 µl of GST, serving as negative control. The remaining 250 µl of the beads were mixed with 1000 µl of the bait molecule (PI3K). Both tubes were then incubated for 40 min at 4 °C on a rotor. Afterwards the samples were washed three times with 1 mL of FISH buffer. Then 100 µl of the GSH-beads bound to GST were incubated with the total cell lysate (for preparation of total cell lysates see 3.4.1) of the destined cell line. Further 100 µl of the GSH-beads bound to GST were incubated with the positive control (20 µg of purified hsERAS). Afterwards the total cell lysate of the destined cell line was added to 100 µl of the GSH-beads bound to PI3K, and 20 µg of purified hsERAS were added to 100 µl of beads bound to PI3K. All samples were then incubated for 1 h at 4 °C on a rotor. Subsequently the samples were washed and centrifuged three times and finally 30 µl of 1x Laemmli buffer were added to the dry beads. The samples were then cooked for 10 min at 95 °C and stored at -80 °C until they were loaded on a SDS-polyacrylamide gel.

Chapter 4

4. Results

Previous studies have shown that the youngest member of the RAS family, Embryonic stem cell- expressed RAS (ERAS) is not only expressed in embryonic stem cells of mice, but also in some human cancer cell lines (Yasuda, Yashiro, Sawada, Ohira, & Hirakawa, 2007). This work focused on the analysis of the expression of ERAS at the mRNA and protein levels in different entities of human cancers by using established cancer cell lines.

4.1 Validation of the qPCR primers

To analyze the expression of ERAS at the mRNA level, two primers were designed by using the software Clone manager, and one primer was ordered, whose sequence was ordered *via* primer design option from NCBI. These primers detect the very N-terminal sequence of *hs*ERAS, which is unique in comparison to the other RAS proteins. All primers were validated regarding their efficiency. Therefore, three different Master mixes were prepared and added to four different concentrations of *hs*ERAS cDNA. Hence, qPCR with SYBR-Green was performed (3.2.4). The data were then processed to gain a standard curve. Furthermore, to examine the possibility of primer-dimer formation or nonspecific binding, the melting curves of the primers were consulted, and the samples of the qPCR were loaded on a 2% agarose gel, after running it. Figure 5 shows the standard curves revealing the efficiency and the respective melting curves, along with the agarose gel scans of this primer validation.

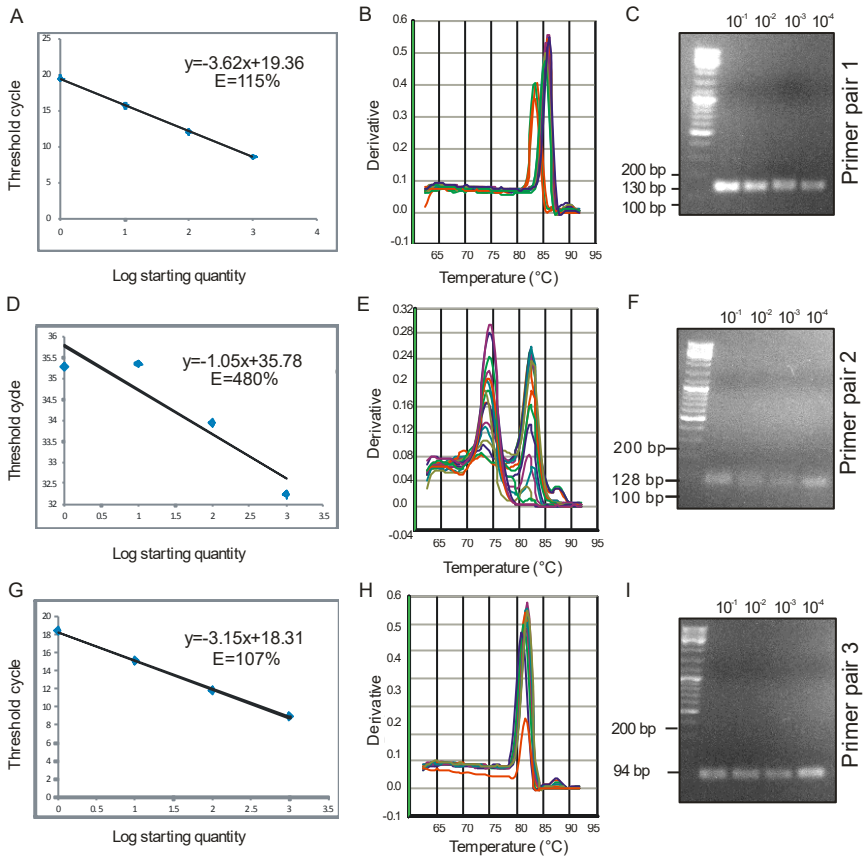

Figure 5: Primer efficiency for 3 different sets of primer.
Standard curve for the first (A), second (D), and third (G) primer along with the melting curves of the first (B), second (E), and third (H) primer as well as 2% agarose gels with qPCR samples of different dilutions (10-1; 10-2; 10-3; 10-4) for the first (C), second (F), and third (I) primer are illustrated.

Figures 5 A, D and G show the standard curves generated with the data derived from the qPCR run. The achieved threshold cycles (CT values) were applied to the coordinate system according to the logarithmic starting quantity of cDNA (concentration of *hs*ERAS cDNA). Subsequently the graph was constructed and the slope was determined, the efficiency was calculated when we use following equation:

$$E = 10^{(-(1/\text{slope}))} - 1$$

While Figures 5 A, D and G showed the described standard curves, Figure B, E and H show the melting curves of the particular qPCR runs with the different primer pairs. Figures 5 C, F and I illustrate the scans of the corresponding 2% agarose gels. The samples of each dilution and the different primer, after running the qPCR, were loaded on the gel (3.3.1).

It can be seen that the efficiencies of the three different sets of primer differ strongly (Figs. 5 A, D and G). The efficiency of the primer should be between 90% and 110%. The only primer pair complying with this criterion was the third primer pair, which showed an efficiency of 107% (Fig. 5G). Thus, the third primer pair seemed to be adequate primer to be used for expression analysis. Melting curve analysis of the qPCR products additionally shows one single peak for the third primer pair (Fig. 5H), indicating that the amplicons are specifically the desired cDNA of *hs*ERAS and no unspecific fragments, such as primer dimers, whereas the melting curve of the second primer pair showed two peaks at two different temperatures revealing formation of primer dimers or non-specific binding. The melting curve for the first set of primers, however, also showed two peaks (Fig. 5B) and, thus, points out that there was also a formation of primer dimers during the qPCR run. Additionally, the agarose gel scans of primer pair one and two showed slight differences in the height of the bands, confirming that a formation of primer dimers occurred (Fig. 5C and F). The expected size of the qPCR product for the first primer pair was about 130bp (Fig. 5C) whereas the expected size of the product for the second primer pair was about 128bp (Fig. 5F). However, the agarose gel scan for the third primer pair shows bands at the expected size of 94bp.

In conclusion, the third primer pair was the most efficient one and therefore used in this thesis for the expression analysis of *hs*ERAS at the mRNA level.

4.2 Validation of the antibody against hsERAS

To analyze the expression of *hs*ERAS at the protein level, a proper validation of an anti-*hs*ERAS antibody against its N-terminus (2.3), was necessary. Therefore, HEK293 cells were transfected with cDNA of *hs*ERAS and other *hs*RAS proteins, such as HRAS, NRAS, KRAS, RRAS, TC21, MRAS and DEXRAS to ensure the specific binding of the antibody against *hs*ERAS (3.3.2). All these proteins were supposed to be expressed with a FLAG-tag in pcDNA3.1 vector. The cells were harvested and lysed (3.4.1). The protein concentrations of the total cell lysates were determined (3.4.2) before performing SDS-Polyacrylamide gel-electrophoresis (3.4.3) followed by Western blotting (3.4.4). The data are shown in Figure 6.

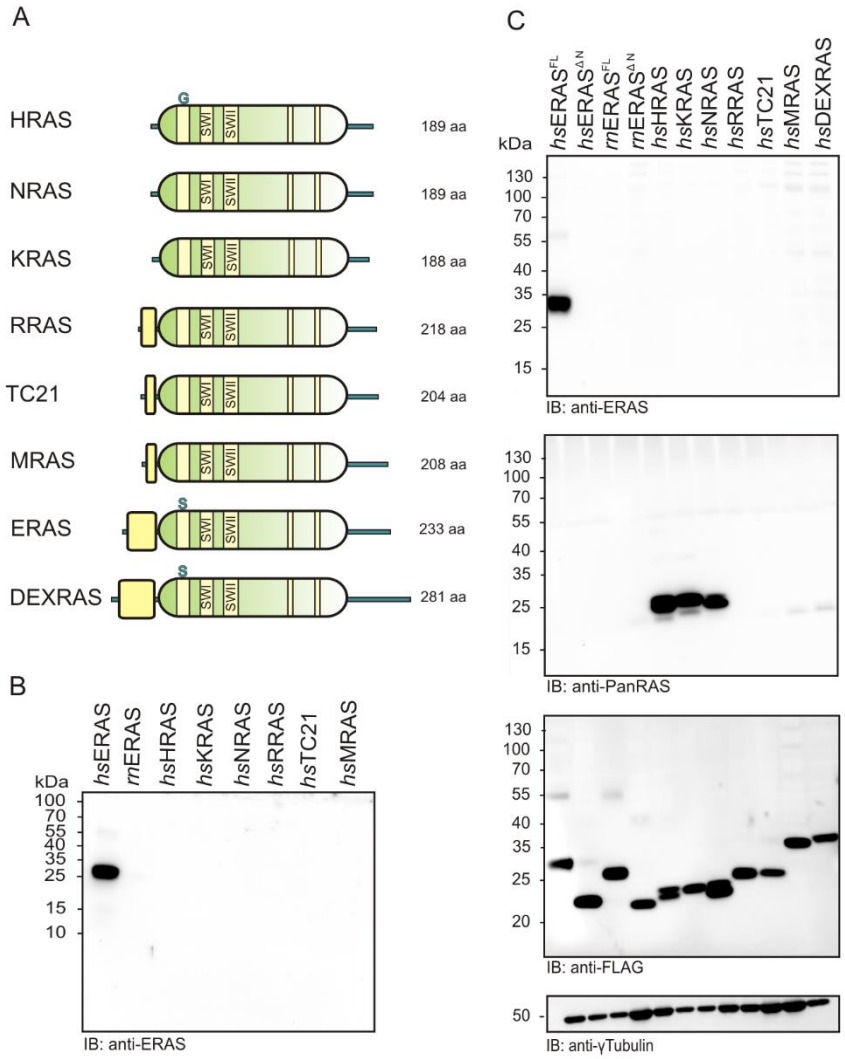

Figure 6: Validation of the anti-hsERAS antibody (sc-51775)
Scheme of the domains of different hsRAS proteins. (B) Immunoblot with purified RAS proteins and anti-hsERAS staining. (C) Immunoblot with HEK cells transfected with different RAS constructs (FLAG-tagged) with anti-hsERAS, anti-PanRAS, anti-FLAG and anti-γTubulin.

Figure 6A shows a scheme of the different domains among the RAS proteins. For the whole antibody validation seven further RAS proteins were used in addition to *hs*ERAS, including HRAS, KRAS, NRAS, RRAS, TC21, MRAS and DEXRAS. On the one hand, this scheme illustrates the similarities of these RAS proteins, such as the five different motives in the G domain (1.3). On the other hand, however, it also shows unique features of ERAS, such as the extended N-terminus and the amino acid deviation within the G1 motif (1.5). As clearly visible *hs*ERAS harbors a length of 233 amino acids and, thus, has a higher molecular weight than the other RAS proteins, due to an extended N-Terminus. The used antibody is supposed to detect the N-Terminus of ERAS. Since the other RAS proteins, except for DEXRAS, do

not harbor such an extended N-Terminus, this antibody should specifically detect *hs*ERAS and no other RAS protein.

Figure 6B shows the scan of the Western blot, performed with cell lysates, containing the above-mentioned RAS proteins, including *rattus-norveticus* ERAS (*rn*ERAS). The scan shows that the antibody only detects *hs*ERAS at the predicted size of 30 kDa. The other RAS proteins are not detectable. The scans of the following blot, shown in Figure 6C emphasize the specificity of this antibody. In this Western blot, in addition to the proteins already used, also cell lysate containing DEXRAS, which also harbors an extended N-Terminus, was used. Furthermore, cell lysates containing mutated variants of *hs*ERAS and *rn*ERAS with deleted N-Terminus (*hs*ERAS$^{\Delta N}$, *rn*ERAS$^{\Delta N}$) were generated for the performance of this Western blot. The Western blot was then performed under the same conditions as the previous one (Fig. 6B). The top scan shows the Western blot with the anti-*hs*ERAS staining. And indeed, the antibody only recognizes hsERAS of full length. Neither *hs*ERAS$^{\Delta N}$ nor *rn*ERAS$^{\Delta N}$ or other RAS were detected. To ensure the cell lysates containing the different proteins were loaded properly on the SDS-Polyacrylamide gels, the blot was stained again with an anti-PanRAS antibody (2.3), which is supposed to mainly detect HRAS, KRAS and NRAS. And we checked the transfection and expression of the all tested FLAG-Tagged RAS isoforms with an anti-FLAG antibody (2.3). Subsequently, the blot was also stained with an anti-γ-Tubulin antibody to visualize that the same protein concentrations were utilized, and, thus, the same conditions for each cell lysate were applied. Collectively, these data allow the conclusion that the anti-*hs*ERAS antibody specifically binds to the N-terminus of *hs*ERAS, and not to other RAS proteins.

Further experiments were executed to guarantee the specificity of the anti-*hs*ERAS antibody. Therefore, HEK293 cells were co-transfected with *hs*ERAS-cDNA and plasmids containing the coding for four different shRNA-constructs against the mRNA of *hs*ERAS (shRNA A-D) and one scrambled shRNA-construct (3.3.2). This plasmid also contains the coding for Green Fluorescent Protein (GFP) to estimate the transfection-efficiency. After that the co-transfected HEK cells were lysed and a portion of them were used for RNA isolation (3.2.1) and qPCR analysis (3.2.4). Afterwards, the rest of the lysate was used for SDS-PAGE (3.4.3) and Western blotting (3.4.4).

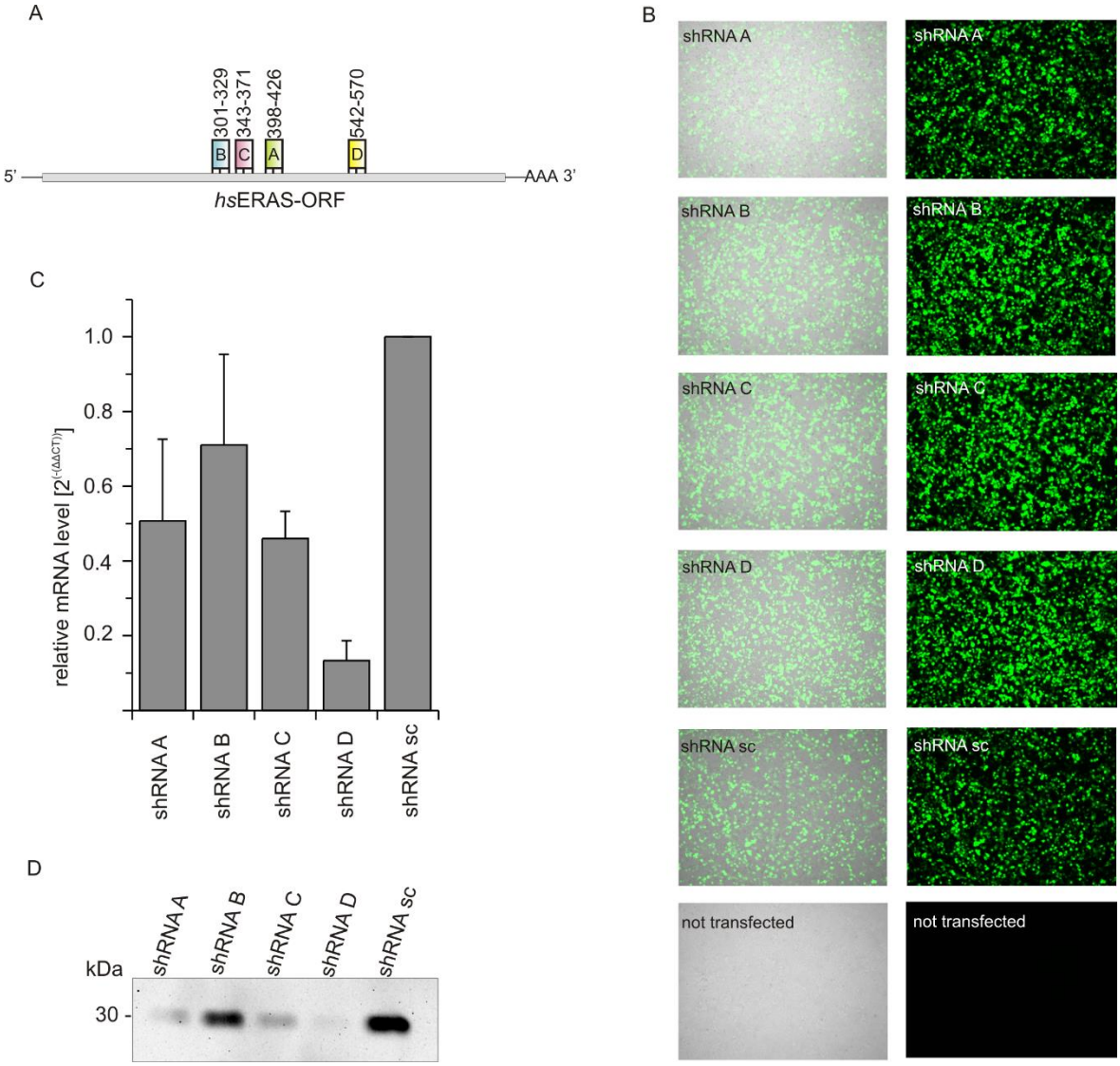

Figure 7: ERAS depletion by specific shRNAs

(A) Scheme of the ORF of hsERAS mRNA, showing the binding sides of the different shRNA constructs (A: 398-426, B: 301-329, C: 343-371, D: 542-572). (B) Images of the co-transfected HEK293T cells (hsERAS and shRNA construct A-D and shRNA sc. shRNA constructs were tGFP-tagged) and not transfected HEK cells, visualized by the tGFP-tag. The transfection efficiency was ~90%. The co-transfection was performed 3 times, the efficiencies were very similar (data not shown). (C) Real-time-PCR data of co-transfected HEK cells show the relative amount of the mRNA of hsERAS in relation to the co-transfection with scrambled (sc) shRNA. The construct D was most efficient in downregulating of the hsERAS mRNA up to 18%. The expression was normalized to the amount of TBP (Mean values with SD, n=3). (D) Immunoblot of the co-transfected HEK cells with anti-hsERAS staining.

Figure 7A shows a scheme of *hs*ERAS' mRNA open reading frame (ORF). Within this scheme, the binding sides of the transfected shRNA constructs are illustrated. Each construction consists of 28 bases, and binds to a distinct region of the mRNA. Exact binding due to perfect complementarity of the shRNA to the mRNA leads to the cleavage of the mRNA molecule. However, imperfect complementarity of the shRNA does not lead to the

cleavage of the mRNA, but to the repression of the translation. Thus, in both cases translation cannot take place, and the protein will not be synthesized, which is shown in Figure 7D. To ensure that the transfection efficiency was equal for each co-transfection, fluorescence microscopic images of the transfected HEK cells were collected (Figure 7B). The transfection efficiency was estimated around 90% for each approach, which guaranteed that following cell-based experiments were underlying the same conditions.

After the co-transfection, RNA samples were isolated and qPCR analysis performed. The data are shown in Figure 7C which shows the relative mRNA level of *hs*ERAS in relation to the approach with the scrambled (sc) shRNA. As one can extract from the graph, all shRNA constructs decrease the expression of *hs*ERAS, but with different efficiencies between 30% (shRNA B) and 82% (shRNA D). Consequently, the shRNA D is the most efficient one, since it downregulates the expression of *hs*ERAS to 18%. This result was reproduced in three repeated experiments under the same conditions as the first one. With these data, the validation of the anti-*hs*ERAS antibody could be extended. Therefore, the co-ntransfected cells were lysed and loaded on a SDS-Polyarcrylamide gel for Western blot analysis. Figure 7D shows a scan of this Western blot. The bands show *hs*ERAS protein at the size of 30 kDa. Each band represents one of the five different approaches with the five different shRNA constructs (shRNA A-D and sc). Since we know that shRNA D is the most efficient and, thus, downregulates the expression of *hs*ERAS most of all and the shRNA B reaches the lowest downregulation (Figure 7C), the antibody should show the weakest signal for shRNA D and the strongest signal for shRNA B (beside shRNA sc). Indeed, the Western blot analysis confirms the qPCR data. Thus, we can say that the anti-*hs*ERAS antibody sc-51775 is highly specific. Just as the qPCR analysis, the Western blot analysis was conducted three times under the same conditions.

4.3 Introduction to the analyzed cell lines

To follow the aim of the work best of all, a broad spectrum of different cancer entities was analyzed. Therefore, 18 cell lines were used, of which 16 have been cultured. The cells were cultured as described in (3.1.1) Because of this, the cultured cell lines are presented and described here.

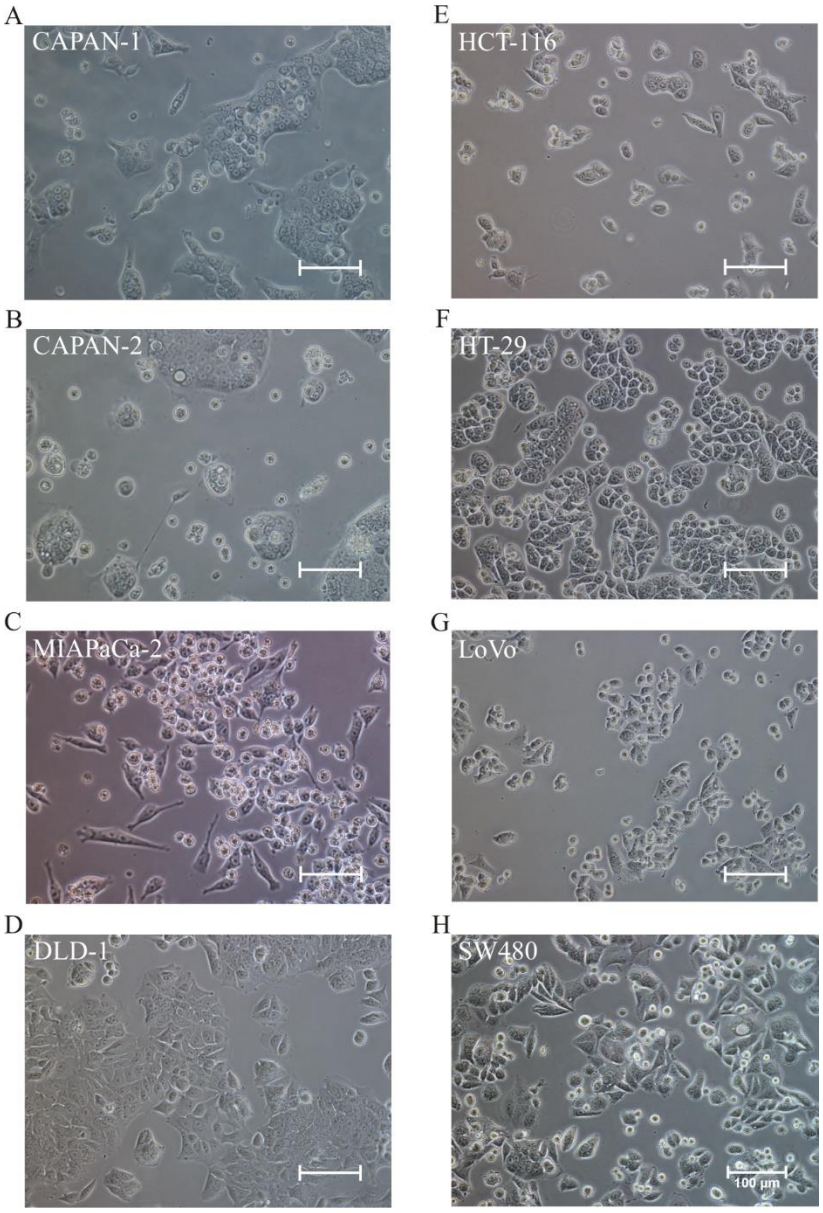

Figure 8: Images of the pancreatic and the colorectal cell lines
Figures (A)-(C) show the analyzed pancreatic adenocarcinoma cell lines. Figures (D)-(H) show the analyzed colorectal cell lines. The scale indicates 100 µm.

Figure 8A shows a picture of the pancreatic adenocarcinoma cell line CAPAN-1. This cell line was derived from a metastasis in the liver of the patient, while the primary tumor was a pancreatic ductal adenocarcinoma (ATCC, CAPAN-1). The cells are rather round shaped and have the tendency to form colonies. Within these colonies, the cells are barely restricted. Furthermore, the cells are growing slowly. In comparison to these cells, the cells of the cell line CAPAN-2 grow faster. They also have the tendency to form colonies, and are round shaped (Fig. 8B). However, these cells were derived from the primary tumor, which was also a ductal pancreatic adenocarcinoma (ATCC, CAPAN-2). The third pancreatic carcinoma

cell line that was examined, is MIAPaCa-2. The cells were derived from the primary tumor (ATCC, MIAPa-Ca-2), being long, and pin shaped (Fig. 8C). MIAPaCa-2 cells are fast growing. Each of the investigated pancreatic cancer cell lines harbor a KRAS mutant variation. CAPAN-1 and CAPAN-2 contain the G12V variant (COSMIC, CAPAN-1) (COSMIC, CAPAN-2), and MIAPaCa-2 the G12C variant (Gradiz, Silva, Carvalho, Botelho, & Mota-Pinto, 2016), which was posted in September 2016 by the National Cancer Institute.

Figures 8D-8H show the colorectal adenocarcinoma cell lines. DLD-1 cells are triangular, well-restricted growing cells (Fig. 8D). Figure 8E shows the colorectal cell line HCT-116, which are triangular shaped and tend to grow in colonies. They grow fast and contain the KRAS mutation G13D (COSMIC, HCTT-116). The next colorectal cell line that was investigated is HT-29, which are small, round shaped cells, growing in colonies (Fig. 8F). They were gained from a primary tumor (ATCC, HT-29). However, these cells are well restricted and grow rather fast. Figure 8G shows the picture of the colorectal cell line LoVo, which were derived from a metastatic lymph node, and are triangular shaped (ATCC, LoVo). In comparison to HT-29, these cells do not tend to form colonies. They rather grow well restricted from each other and fast. The cells have the KRAS G13D mutation (COSMIC, LoVo). The last colorectal cancer cell line, that was examined is SW480. These cells were gained from a primary tumor (ATCC, SW480) and growing well restricted (Fig. 8H) and fast. These cells also harbor a KRAS G12V mutation (COSMIC, SW480).

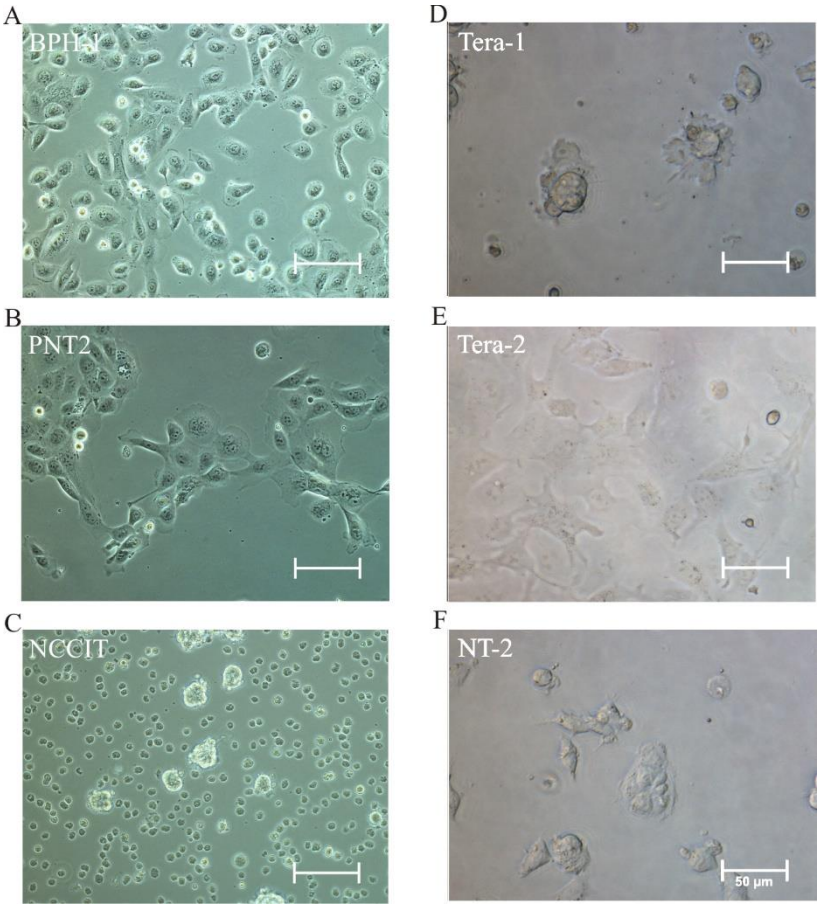

Figure 9: Images of the prostate and teratocarcinoma cell lines
Figures (A) and (B) show images of the analyzed prostate cell lines, while BPH-1 is a cell line of a benign prostatic hyperplasia, and PNT2 are immortalized normal adult prostatic epithelial cells. Figure (C) shows tumorigenic placenta cells, while Figures (D)-(F) show teratocarcinoma cell lines. The scale indicates 50 µm.

Figures 9A and 9B show images of prostatic cells. BPH-1 are benign prostatic hyperplasia cells. In contrast to the cell lines already described, this cell line is not a cancer cell line. These cells were derived from a benign prostate tumor, and, thus, did not transform (DSMZ, BPH-1). This cell line was especially investigated in this study to analyze the expression of *hs*ERAS in benign tumor cells to compare it then to normal prostatic cells (PNT2). BPH-1 cells are epithelial cells, which grow in monolayers. In comparison to the other investigated prostatic cells, BPH-1 cells grow faster. However, in this study, also normal prostatic cells were investigated concerning the expression of *hs*ERAS. This cell line was PNT2, which were derived from a healthy prostate, and immortalized (Public Health England, PNT2). Within the scope of this study, we were interested in understanding how the expression-level of *hs*ERAS of tumor- and non-tumor cells of the same organ differs.

Figure 9C shows NCCIT cells which are tumorigenic placenta cells. These cells are very small, round shaped cells, which grow in clusters. Interestingly these cells are pluripotent cells (ATCC, NCCIT). Thus, they can differentiate into all cells of the three different germ layers. Figure 9D is an image of the teratocarcinoma cell line Tera-1 which were gained from a metastasis in the lung, while the primarily affected tissue was the testis (ATCC, Tera-1). The cells grow fast and in layers. Figure 9E shows Tera-2 cells. They are also testicular germ cell tumor cells and were derived from a lung metastasis (ATCC, Tera-2). However, these cells are larger than the Tera-1 cells, but grow more slowly. A subline of Tera-2, NTERA-2 (NT-2) was also cultured and investigated in this study. These cells are pluripotent cells (ATCC, NTERA-2). They grow fast and also in layers. NT-2 cells have an epithelial-like morphology, a prominent nucleus and nucleoli (Figure 9F). Since teratocarcinoma cells are malignant germ cells, also called embryonal carcinoma cells, these cells are suggested to be the malignant correspondent to embryonic stem cells (Andrews, 2002). Since ERAS was found in undifferentiated embryonic stem cells (see 1.5), it was interesting to analyze whether *hs*ERAS is expressed in such malignant germ cells.

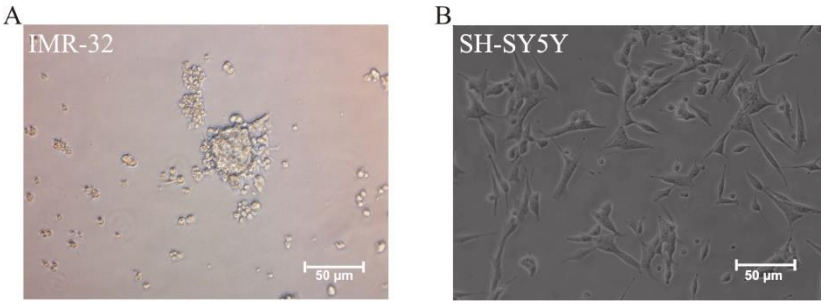

Figure 10: Images of neuroblastoma cell lines
Figures (A) and (B) show the analyzed neuroblastoma cell lines IMR-32 (A) and SH-SY5Y (B). The scale indicates 50 µm.

Furthermore, two neuroblastoma cell lines were investigated, including IMR-32 and SH-SY5Y. The cell line IMR-32 was derived from an abdominal metastasis of a neuroblastoma (ATCC, IMR-32). These cells are very small, round shaped cells, growing in patches (Fig. 10A). The other cell line was SH-SY5Y, which form clusters. The cells around these clusters exhibit extensions reminding of neurites. These cells are a subline of the neuroblastoma cell line SK-N-SH (ATCC, SH-SY5Y).

Moreover, two glioblastoma cell lines U87MG and A172 were included in this study. However, the cell lines were cultured by our collaborator Prof. Dr. Guido Reifenberger (Institute of Neuropathology, University Hospital Düsseldorf), who provided us with cell pellets.

4.4 Expression of hsERAS in the different cell lines

The expression analysis was performed in two different steps. Firstly, RNA was isolated from cell lines described above (3.2.1). In the next step, the isolated RNA was treated with DNase (3.2.2) and afterwards cDNA was synthesized (3.2.3) to determine finally the *hs*ERAS mRNA expression by conducting qPCR (3.2.4). Therefore, the validated primer pair three was used (5.1). Secondly, the expression of *hs*ERAS at the protein level was investigated. Therefore, total cell lysates of the cell lines were prepared (3.4.1) and their protein concentration determined (3.4.2). 75 µg of each lysate was analyzed by SDS-PAGE (3.4.3) and subsequent Western blotting (3.4.4) when an anti-*hs*ERAS antibody was used validated in this study.

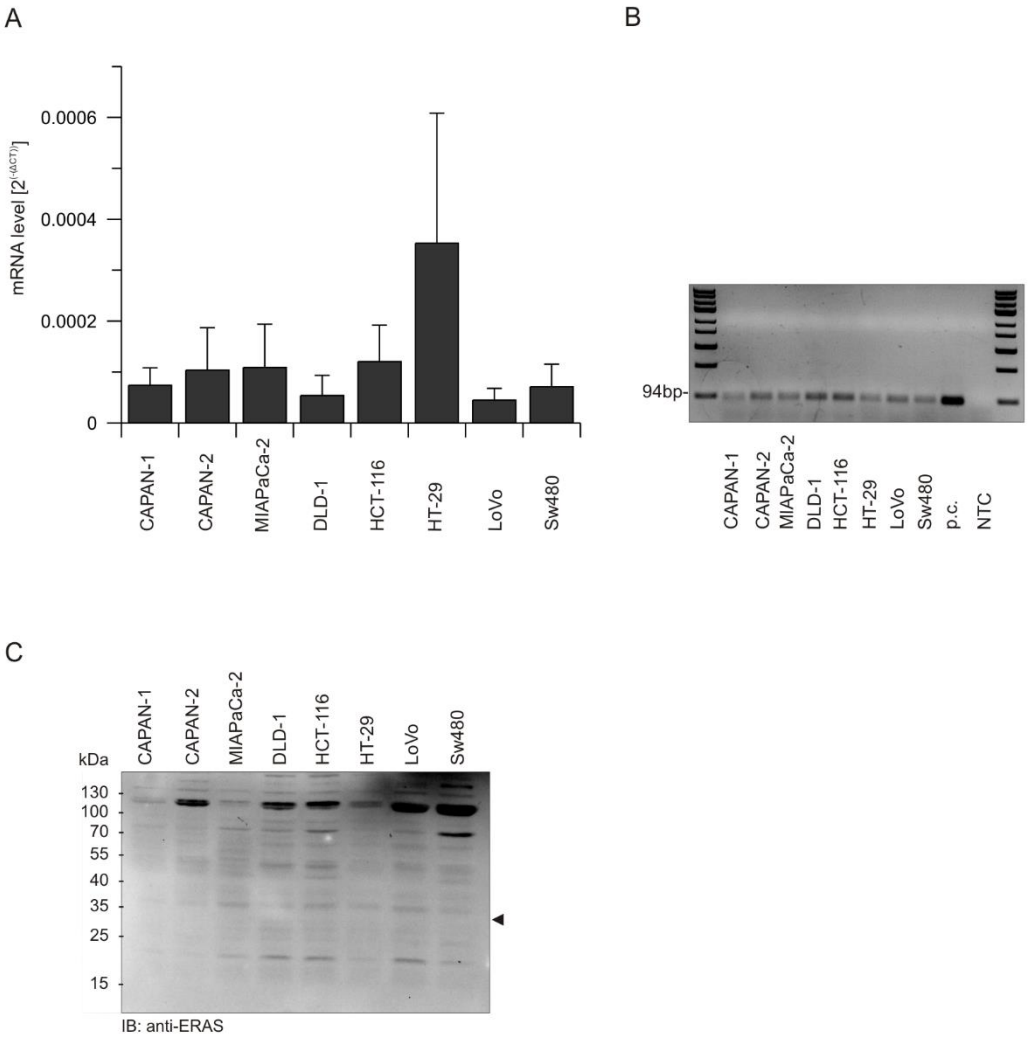

Figure 11: Expression of hsERAS in pancreatic and coloractal cancer cells
(A) Real-time-PCR analysis of the pancreatic cancer cell lines CAPAN-1, CAPAN-2, MIAPaCa-2, and the colorectal cell lines DLD-1, HCT-116, HT-29, LOVO and SW480. Shown is the expression of hsERAS at the mRNA level, normalized to the amount of TBP (Mean values and SD, n=3). (B) 2% agarose gel with Real-time-PCR samples of the pancreatic and colorectal cancer cell lines, showing the amplified mRNA of hsERAS (p.c.= positive control cDNA of hsERAS diluted 1:1000; NTC= non-template control). (C) Immunoblot of the cell lines CAPAN-1, CAPAN-2, MIAPaCa-2, DLD-1, HCT-116, HT-29, LoVo, and SW480 with anti-hsERAS staining (molecular weight of hsERAS = 30kDa).

Figure 11A illustrates the expression of *hs*ERAS at the mRNA level in the pancreatic adenocarcinoma and the colorectal cancer cell lines including the corresponding standard deviations (SD). Therefore, the CT (cycle of threshold) values that were determined by qPCR were related to the CT values of the reference gene TBP (TATA-Box Binding Protein). The CT value correlates to the qPCR cycle in which the fluorescence signal exceeds a certain threshold value. The mRNA level of the different cell lines was then calculated when this formula was used: $2^{(-(\Delta CT))}$. For each qPCR run and each cell line triplicates were

prepared, and the Mean CT values were determined. The whole experiment was repeated three times (n=3) under the same conditions (biological replicates). After running the qPCR, the samples were loaded on a 2% agarose gel and visualized (3.3.1) to ensure that no primer dimers were formed during the qPCR run. Figure 11B shows a scan of the agarose gel belonging to the pancreatic and colorectal cell lines. In this figure there is one single band for each cell line at the size of 94 bp discernible. This size is the expected size of the amplicons according to the chosen primer pair (5.1, Fig. 5I). Thus, no primer dimer formation happened during the qPCR run and the results in Figure 11A are reliable. In Figure 11A is visible that MIAPaCa-2 expresses *hs*ERAS at the mRNA level out of the pancreatic adenocarcinoma cell lines the most (0.00011), while the expression of *hs*ERAS in CAPAN-1 is the lowest out of the pancreatic cell lines (0.0007), and CAPAN-2 expresses less than MIAPaCa-2, but more than CAPAN-1 (0.0001). However, the highest expression of ERAS, out of the colorectal cancer cell lines, has HT-29 (0.00035), followed by HCT-116 (0.00012), SW480 (0.0007), DLD-1 (0.000053), and LoVo (0.00005). In conclusion HT-29 expresses *hs*ERAS the most, out of all cell lines showed in Figure 11. Hence, this cell line should also show the strongest band in the Western blot, which would correlate with the highest expression at the protein level. However, the associated Western blot (Figure 11C) shows no bands at all at the predicted size of 30 kDa coming up to the molecular weight of *hs*ERAS. Strong bands in top of the blot, (between 130 and 100 kDa) though, are unspecific bands.

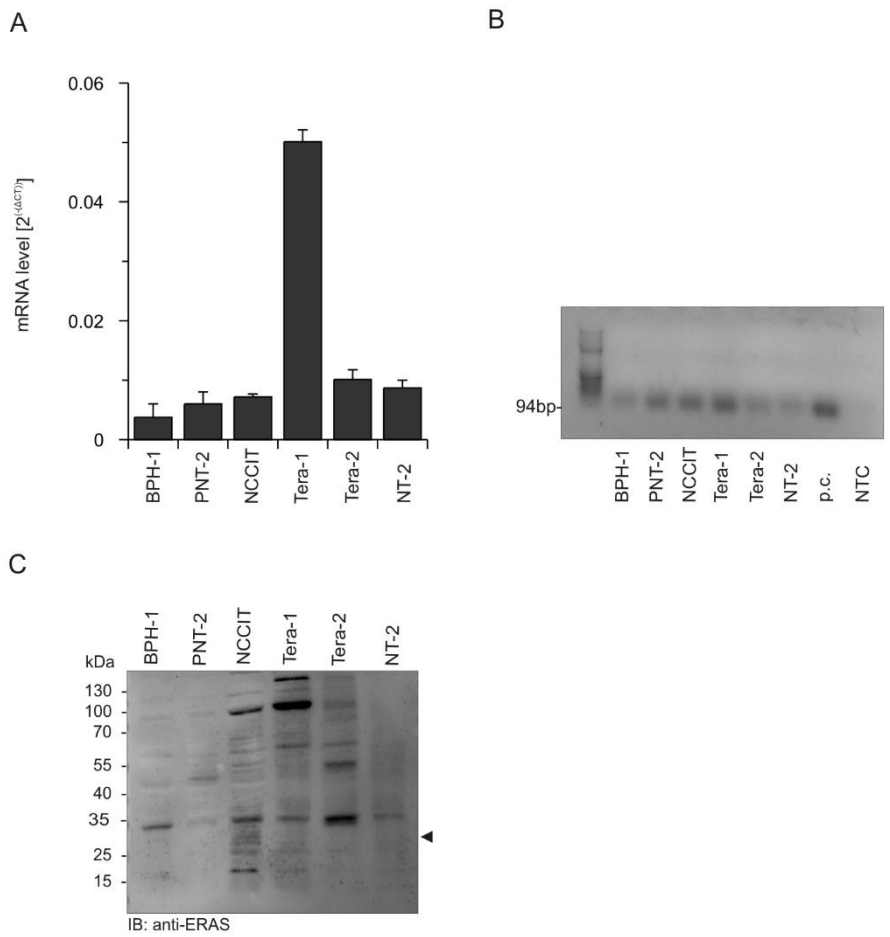

Figure 12: Expression of hsERAS in prostatic and teratocarcinoma cells
(A) Real-time-PCR analysis of the prostate cell lines BPH-1 and PNT-2, and the teratocarcinoma cell lines NCCIT, Tera-1, Tera-2, and NT-2. Shown is the expression of hsERAS at the mRNA level, normalized to the amount of TBP (Mean values and SD, n=3). (B) 2% agarose gel with qPCR samples of the prostate and teratocarcinoma cell lines, showing the amplified mRNA of hsERAS (p.c.= positive control cDNA of hsERAS diluted 1:1000; NTC= non-template control). (C) Immunoblot of the cell lines BPH-1, PNT-2, NCCIT, Tera-1, Tera-2, and NT-2 with anti-hsERAS staining. Themolecular weight of hsERAS is 30kDa.

Figure 12A shows the *hs*ERAS mRNA levels of the cell lines BPH-1, PNT-2, Tera-1, Tera-2 and NT-2. These data were generated and processed as described above. Figure 12B illustrates the scan of the agarose gel that was loaded with the qPCR samples. Only one single band at the predicted size of 94 bp for each cell line was visible, proving that there was no primer dimer formation. Interestingly, it is clearly discernible that especially the teratocarcinoma cell lines Tera-1, Tera-2 and NT-2 express the mRNA of *hs*ERAS most of all. Important for the evaluation and analysis of these data is the fact that the scaling of this graph is different as compared to the scaling of the graph in Figure 11A, which shows that the colorectal carcinoma cell line HT-29 expresses *hs*ERAS in a high level (0.00035).

However, the teratocarcinoma cell lines express the mRNA in a much higher level than HT-29 does. It must be pointed out here that the cell line Tera-1 expresses the mRNA of *hs*ERAS most of all(0.05), followed by Tera-2 (0.011), and NT-2 (0.008). Close to these expression levels, the mRNA is also expressed by the NCCIT cells (0.0075). The cell line BPH-1 has rather low levels of the ERAS mRNA (0.0037), whereas the other prostatic cell line PNT-2 expresses more of the *hs*ERAS mRNA (0.006). These cell lines, though, express more of the mRNA than HT-29. The expression analysis at the protein level was performed for these cell lines as well, which is represented in Figure 12C. This figure shows the scan of the Western blot that was performed with the prostatic, teratocarcinoma cell lines and NCCIT. According to the high levels of mRNA, especially in the Tera-1, Tera-2 and NT-2 cells, this blot was expected to show bands at the predicted size of 30 kDa. However, there is no band visible at the size of 30 kDa, revealing that these cells also do not synthesize the ERAS protein.

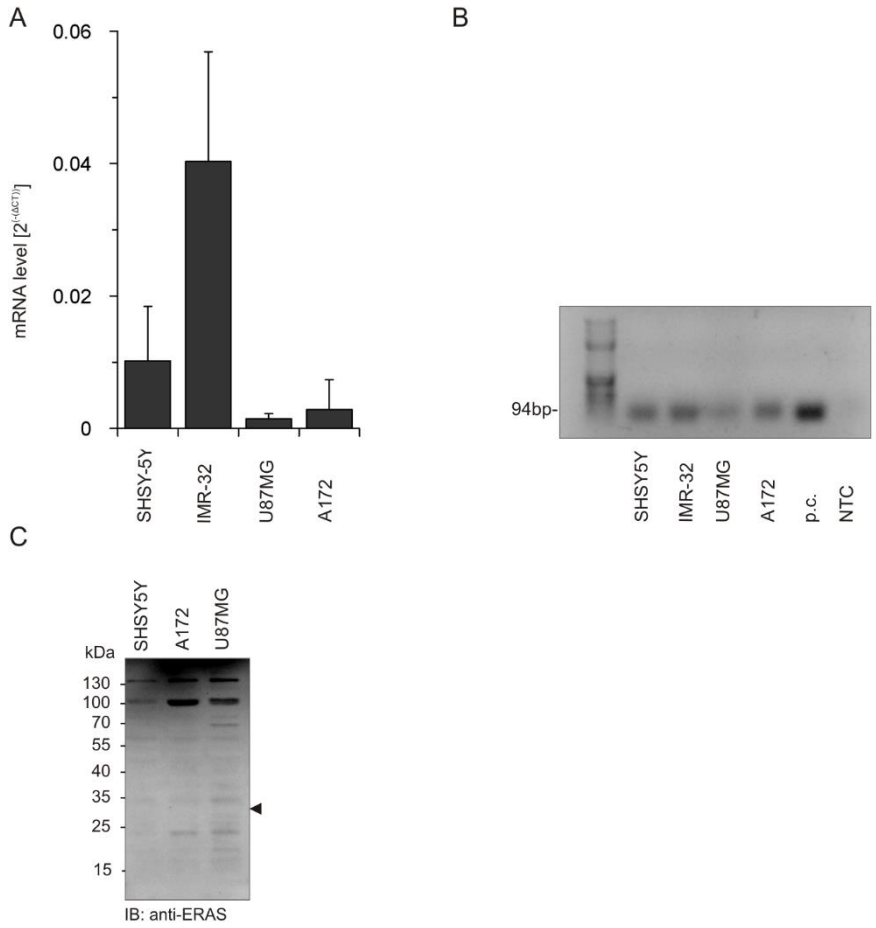

Figure 13: Expression of hsERAS in neuroblastoma and glioblastoma cells
(A) qPCR analysis of the neuroblastoma cell lines SH-SY5Y and IMR-32 and the gioblastoma cell lines U87MG and A172. You can see the expression of hsERAS at the mRNA level, normalized to the amount of TBP (Mean values and SD, n=3). (B) 2% agarose gel with Real-time-PCR samples of the neuroblastoma and glioblastoma cell lines, showing the amplified mRNA of hsERAS (p.c. = positive control cDNA of hsERAS diluted 1:1000; NTC= non-template control). (C) Immunoblot of the cell lines SH-SY5Y, A172, and U87MG with anti-hsERAS staining (molecular weight of hsERAS = 30kDa).

Figure 13A illustrates the mRNA levels of the glioblastoma (U87MG, A172) and neuroblastoma (SH-SY5Y, IMR-32) cell lines, while 13B shows the scan of the control agarose gel. In 13B it is obvious, that again only one single band at the size of 94bp for each cell line is visible, manifesting the absence of primer dimers. Thus, the mRNA levels shown in Fig. 13A are reliable, which shows that the neuroblastoma cell lines IMR-32 (0.04) and SH-SY5Y (0.01) have higher amounts of *hs*ERAS mRNA than the glioblastoma cell lines U87MG (0.0025) and A172 (0.007). Protein analysis revealed that also these cell lines do not synthesize *hs*ERAS, as no band at the size of 30 kDa is visible (Fig. 13C). Protein

analysis of the cell line IMR-32 could not be performed, due to a very low protein concentration.

It can be concluded from the data described above that *hs*ERAS is expressed in several different human tumor and cancer cell lines but the ERAS protein was hardly detectable.

GST-Pull-down-Assay

To verify ERAS at the protein level, a GST-Pull-down-Assay was performed to collect ERAS-enriched samples. In this context, the cell lines with the highest ERAS mRNA levels according to the qPCR-analysis were examined in detail. These cell lines were neuroblastoma cell lines SH-SY5Y, IMR-32 and the teratocarcinoma cell lines Tera-1, Tera-2 and NT-2 were chosen for this experiment.

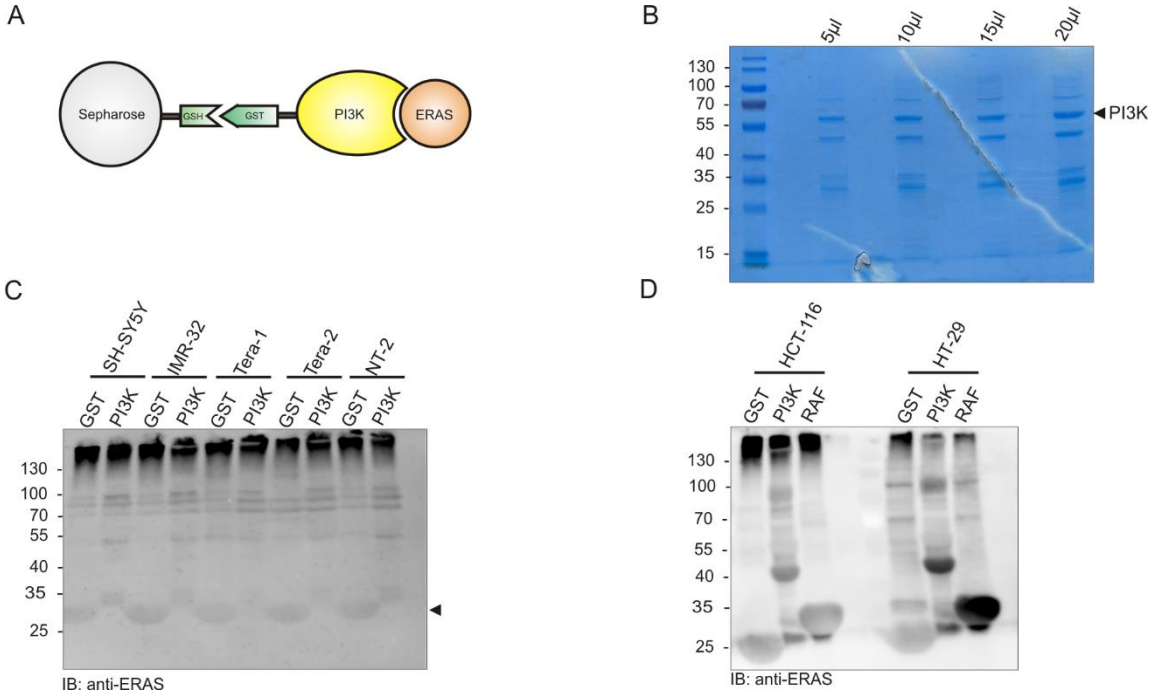

Figure 14: Pull-down analysis of ERAS protein by GST-PI3K blot

(A) Scheme of the GST-Pull-down assay illustrates bead-coupled GST-PI3K, which is able to bind tightly ERAS and pull it down by centrifugation. (B) Different amounts of E. coli lysates expressing GST-PI3K (5 µl to 20 µl) were analyzed by SDS-PAGE gel stained with Coomassie brilliant blue. The arrow head points to the protein band of PI3K. (C) Western blot analysis of the Pull-down samples were obtained by mixing 20 µl lysates containing GST-PI3K or GSTwith lysates of the neuroblastoma cell lines (SH-SY5Y, IMR-32) and the teratocarcinoma cell lines (Tera-1, Tera-2, NT-2). (D) Western blot analysis of the Pull-down samples were obtained by mixing 20 µl lysates containing GST-PI3K GST-RAF or GST with lysates of the colorectal carcinoma (HCT-116, HT-29). The SDS-PAGE and Western blot analysis was stained with the anti-hsERAS antibody (1:750). The arrowhead brings out the predicted size of ERASD at 30 kDa (C).

Figure 14A describes the principle of the performed Pull-down experiment. To detect even slight amounts of *hs*ERAS, a bait-molecule coupled to GST is needed. In this case PI3K was chosen, which has been shown to bind tightly to ERAS (Nakhaei-Rad et al., 2016). When this GST-PI3K protein is incubated with a GSH-Sepharose bead, the GST binds to GSH. When the cell lysate containing the target protein such as the cell lines expressing ERAS is now incubated with lysates with GST-PI3K or GST, which were generated in *E. coli* (3.4.6). Centrifugation leads to the pull-down of the ERAS proteins. To test the amounts of GST-PI3K in the *E. coli* lysates, different volumes of the lysate (5 µl to 20 µl) were loaded on an SDS-polyacrylamide gel. The gel was stained with Coomassie brilliant blue. Figure 14B shows the increasing amount of PI3K pointed out by the arrowhead). 20 µl of generated GST-PI3K und GST lysates was then used for the Pull-down-assay. Two different tubes were prepared for each cell line lysates of the cell lines SH-SY5Y, IMR-32, Tera-1, Tera-2 and NT-2. One was incubated with GST lysate, serving as negative control, and the other was incubated with the GST-PI3K. After the Pull-down experiment, the samples were loaded on a gel, and Western blotting was performed. The results are represented in Figure 14C. At the size of 30 kDa no band is visible for any of the investigated cell lines, indicating that the *hs*ERAS mRNA is not translated in human cancer cells. Furthermore, the Pull-down assay was performed with the lysates of the cell lines HCT-116 and HT-29. However, in this experiment a further bait-molecule, RAF, was used. The results are represented in Figure 14D.

Chapter 5

5. Discussion

It is known that RAS proteins play crucial roles in intracellular signaling processes, such as transcription, survival, growth, proliferation and differentiation (Castellano & Santos, 2011). Certain oncogenic RAS proteins (HRAS and KRAS) were found in more than 30% of human cancer entities (Papke & Der, 2017). Thus, they represent appreciable targets for oncogenic activation (Castellano & Santos, 2011; Pylayeva-Gupta, Grabocka, & Bar-Sagi, 2011). A novel member of this family, ERAS, is regulated at the transcriptional level and act as an oncogene without requiring any mutation. Some human cancer cell lines have been reported to express ERAS. However, there is a lack of information about the impact of ERAS in other human cancers. Therefore, the ERAS expression was investigated in different human cancer cell lines with different origins. The amount of ERAS expression in reported cell lines was compared with new cancer cells of the present study. With the help of this work, it could be shown that different cancer entities express *hs*ERAS mRNA in different levels. Interestingly, remarkable amounts of ERAS were detected in human embryonal carcinoma cells which may be related to the function of ERAS in stem cells survival.

5.1 Different cancer entities show different hsERAS mRNA levels

ERAS is the novel member of the RAS family whose expression was firstly reported in undifferentiated embryonic stem cells (ESCs) of mice (Takahashi, Mitsui, & Yamanaka, 2003). ERAS has clearly to be distinguished from the other RAS family members based on its unique sequence highlights, the extended N-terminus and the serine 50 instead of glycine (HRAS, G12) within the G1 motif, making it GAP insensitive and therefore hyperactive (Nakhaei-Rad et al., 2015). The substitution of glycine 12 to any other residues makes RAS proteins hyperactive. This oncogenic mutation of RAS is found in human cancers (Pylayeva-Gupta, Grabocka, & Bar-Sagi, 2011). So it is interesting to clarify whether ERAS, like hyperactive RAS proteins (HRAS, KRAS, NRAS) that were found to correlate to cancer development, takes a role in human cells and especially in human ESC and human cancer cells (Bos, 1989; Pylayeva-Gupta, et al., 2011). Earlier studies have failed in detecting ERAS in human ESC. Kameda and colleagues have explained that this is due to the upstream premature polyadenylation signal within the human ERAS locus (Kameda & Thomson, 2005). Later, Yasuda and coworkers have described the expression of *hs*ERAS in certain human cancer cell lines including colorectal (HCT-116, DLD-1, LS174T and HT-29),

pancreatic (RWP-1 and MIAPaCa-2), and breast carcinoma (AMB-231) cells (Yasuda, Yashiro, Sawada, Ohira, & Hirakawa, 2007). Nevertheless, this group have only examined the expression of *hs*ERAS mRNA and not of the protein itself. However, they have performed a conventional reverse-transcriptase (RT-) PCR and, therefore, not quantified the mRNA levels. As an internal control, they have used GAPDH. The present study, however, investigated various housekeeping genes, including GAPDH, TBP, HPRT, SDHA, to ensure that all examined cell lines show the same expression levels of the housekeeping genes. So the amount of the hsERAS mRNA was not only quantified by performing q-PCR, but also the mRNA amounts were compared within the 18 different cell lines.

In 2009, Kaizaki and colleagues have investigated the expression of ERAS in human primary gastric carcinoma of 381 different patients who have not undergone a therapy so far. This group has manufactured an anti-*hs*ERAS antibody and has performed both immunohistochemical staining and conventional RT-PCR. They have shown that ERAS was expressed in 44% of these samples, while ERAS mRNA was detected in 45% of the samples (Kaizaki et al., 2009). They have proposed that ERAS plays a role in gastric tumorigenesis since early stage gastric tumors express it more frequently than advanced stages. Furthermore, they reported that ERAS-positive patients have a significantly better overall survival than ERAS-negative patients, while ERAS is not supposed to be an independent factor for survival. However, no internal control was used for the PCR analysis. Moreover, the manufactured antibody which has not been validated was supposed to detect *hs*ERAS at the molecular weight of 25 kDa. The specificity of the antibody, however, was not shown, whereas the specificity of the antibody used in this study was examined. In the present study, *hs*ERAS protein was detected at 30 kDa and rat ERAS at 25 kDa. Furthermore, previous studies concerning *hs*ERAS have not shown the validation of the used antibodies, thus their specificity remains unclear.

Yashiro *et al*. have investigated the expression of *hs*ERAS mRNA in 15 different human gastric cancer cell lines (Yashiro, 2009). For this reason, they have used conventional RT-PCR and GAPDH as an internal control. Scans of the agarose gels showed that 8 out of the 15 different gastric cancer cell lines express *hs*ERAS mRNA, while the ERAS DNA was found in all these cell lines. However, a positive control was not included in this PCR analysis. They have treated the other 7 gastric cancer cell lines, not expressing the ERAS mRNA, with 5 µM of 5-aza-CdR (inhibitor of DNA methyltransferase), to check the

epigenetic regulation of the ERAS gene. According to their results, all 7 gastric cancer cell lines expressed the ERAS mRNA after the 5-aza-CdR treatment. However, a correlation of the ERAS expression and the expression of different DNA methyltransferases was not seen. Four days after the treatment, ERAS mRNA expression was silenced again revealing that the underlying epigenetic regulation may be reversible. Therefore, they have concluded that ERAS might take a crucial role within gastric tumorigenesis and in charge of cancer stem cell-like characters (Yashiro et al., 2009).

Meantime the group of Tanaka have seen a possibility of improving models for human ESC-based therapy in using cynomolgus monkey ESC instead of mice ESC. They did neither find ERAS mRNA in cynomolgus monkey ESC nor in adult tissues, especially in liver, brain and kidney (Tanaka et al., 2009). Based on this and immunohistochemical analysis they have concluded that differentiated mouse ESC did not express ERAS any longer (Takahashi, Mitsui, & Yamanaka, 2003). They next investigated the expression of ERAS in cynomolgus ES cell-derived neurons and teratoma cells. This experiment has finally shown that these cells express ERAS mRNA at high levels. However, after transplanting the teratoma cells in NOG mice, no tumor was formed which led the group to the conclusion that ERAS does not contribute to the tumorgenicity of cynomolgus cells (Tanaka et al., 2009).

Interestingly, Aoyama and coworkers have shown in 2010 that ERAS is endogenously expressed in human neuroblastoma cells (SH-SY5Y) and might be important for the development of neuroblastoma. For reasons of low expression, they have overexpressed ERAS in the neuroblastoma cell line SH-SY5Y and analyzed the proliferation rate and the survival of the cells when exposed to commonly used chemotherapeutic agents. The mRNA expression was visualized by performing conventional RT-PCR, and the ERAS protein was visualized by Immunoblotting (Aoyama et al., 2010). The results showed that proliferation did not significantly increase in ERAS overexpressing cells, compared to the parental cell line (Aoyama, 2010). However, the survival rate of ERAS overexpressing cells was significantly higher than the survival rate of the parental cell line, showing that ERAS increases the resistance to chemotherapy, most likely via the PI3K-AKT pathway.

As described, previous studies have shown that *hs*ERAS is expressed in some human cancer cell lines. However, these groups did not quantify the amounts of *hs*ERAS mRNA.

Furthermore, they used colorectal, pancreatic, esophageal and breast cancer cell lines (Yasuda, Yashiro, Sawada, Ohira, & Hirakawa, 2007), and neuroblastoma cell lines (Aoyama, 2010). The present study extended the expression analysis and included prostate, teratocarcinoma, and glioblastoma cell lines. Therefore, three different sets of primer were thoroughly validated and the expression of different housekeeping genes, GAPDH, TBP, HPRT, SDHA, within all of the investigated cells were analyzed to ensure that the internal control we have used are suitable for not only quantifying the ERAS mRNA, but also for comparing the different expression levels of all cancer cells. So the present study not only reveals the expression levels of the newly included cell lines, but has also found cancer entities, expressing higher ERAS mRNA levels (Figures 11-13). While Yasuda et al. postulated in 2007 that especially colorectal cancer cell lines, followed by pancreatic cancer cell lines express high amounts of *hs*ERAS mRNA, the present work shows that contrary to the pancreatic cancer cell lines, the colorectal cancer cell lines significantly differ in their ERAS expression (Fig. 11). However, the highest amount of *hs*ERAS mRNA was found in teratocarcinoma and neuroblastoma cell lines (Fig.12-13). Probably the presence of *hs*ERAS and *hs*ERAS mRNA depends on the state of carcinogenesis. This hypothesis is underlined by the fact that the group of Yasuda et al. have shown that the expression of ERAS is not constitutively stable and can be silenced (Yasuda, Yashiro, Sawada, Ohira, & Hirakawa, 2007). Consequently, any cancer cell might need ERAS at some point and might express *hs*ERAS during carcinogenesis. Furthermore, an explanation for the different expression amounts of *hs*ERAS is that it is rather required by undifferentiated cells such as teratocarcinoma cell lines with the highest amounts of *hs*ERAS mRNA. In addition, ERAS is expressed in undifferentiated embryonic stem cells of mice (Takahashi, Mitsui, & Yamanaka, 2003), and obviously plays a crucial role in the maintenance of stem cell-like properties in rat hepatic stellate cells (Nakhaei-Rad et al., 2016), underlining the hypothesis that ERAS may only be expressed in adult stem cells.

5.2 High amount of mRNA, but low amount of protein

To analyze endogenous proteins there is need of validated antibodies. From three different antibodies which were commercially available, the antibody (Anti-hsERAS sc-51077) that was against the unique ERAS N-terminus was validated in the present study. Using various purified RAS proteins and overexpressed RAS genes in HEK cells has shown that the antibody Anti-hsERAS sc-51077 specifically recognized human ERAS (Fig. 6). Western blotting analysis of human cancer cells in this study using the antibody showed very faint

protein bands at 30 kDa, due to a strong background, even in the cell lysates from the teratocarcinoma cell lysate (Fig. 11-13). Kubota et al have reported a detection of the ERAS protein in certain human gastric cancer tissues at the size of 24 kDa (Kubota et al., 2010), which is much smaller than the expected molecular weight of 30 kDa. It remains unclear whether the reported protein really is the ERAS protein. In the present study, GST-PI3K, which tightly binds ERAS, was used to pulldown ERAS proteins from the cell lysates. Pulldown analysis of the cell lysates of SH-SY5Y and IMR-32 neuroblastoma cell lines, Tera-1, Tera-2, and NT-2 teratocarcinoma cell lines, and also the HCT-116 and HT-29 cell lines did not clearly show the ERAS proteins at the expected molecular weight of 30 kDa (Fig. 14). HCT-116 and HT-29 cell lines showed, however, protein bands not only at 30 kDa, but also at 50 and 110 kDa, respectively. Large amounts of the ERAS protein were expected especially in Tera-1, Tera-2 and NT-2, due to the large mRNA amounts detected in the present study. It seems that ERAS is expressed at the mRNA level and might be synthesized in some tumor cell lines at a very low extent, however, and hence is very difficult to detect. A possible mechanism negatively regulating translation may be the presence of miRNA (He & Hannon, 2004). Another mechanism may be the formation of stress granules, counteracting translation of *hs*ERAS mRNA (Protter & Parker, 2016). Notably, a serine at position 50 in *hs*ERAS instead of a glycine (Fig. 3) makes it GAP insensitive and hence hyperactive (Nakhaei-Rad et al., 2015). Consequently, even very low amounts of the ERAS protein may be crucial in cell signaling (Nakhaei-Rad et al., 2016).

5.3 Functions of hsERAS

The functions of *hs*ERAS in cancer cells is not clear yet. However, ERAS has firstly been found in undifferentiated embryonic mouse cells and introduced to take crucial role in the maintenance of tumor-like properties (Takahashi, Mitsui, & Yamanaka, 2003). Furthermore, it was reported that ERAS facilitates the reprogramming of somatic cells to induced pluripotent stem cells via the ERAS-AKT signaling pathway (Yu et al., 2014). Yu et al. have suggested in this context that the described molecular basis of somatic reprogramming is also a principle of cancer initiation. Above this, *hs*ERAS was found in gastric cancer and described to take role in proliferation and metastasis (Wei, 2013). However, it was also reported that ERAS expression does not correlate with the histological differentiation of the cancer cells (Kubota et al., 2010; Wei, 2013). Additionally, ERAS expression was shown in human neuroblastoma cell lines and related to chemotherapy resistance. Furthermore,

expression of ERAS is proved to be important for the maintenance of stem cell-like properties in rat hepatic stellate cells (Nakhaei-Rad et al., 2016). However, the data obtained in the present study show that especially the teratocarcinomas express ERAS in high amounts. Teratocarcinomas are known to comprise undifferentiated embryonal carcinoma-cell components. Embryonal carcinomas have been reported to be part of the first demonstration of cancer stem cells (Kleinsmith & Pierce, 1964). One of the investigated teratocarcinoma cell lines, NT-2, is formally known to be a pluripotent cell line. This cell line is expressing ERAS at high amounts (Fig.12), leading to the conclusion of ERAS might be important for maintenance of stem cell like properties such as pluripotency.

5.4 Role of ERAS in carcinogenesis

Since ERAS was found in undifferentiated cells and also in human cancer cells, one may suppose ERAS to play a critical role in these cells. Several groups have reported a role of ERAS in human cancer cells. Aoyama and coworkers have published that ERAS does not increase the proliferation rate, but the survival rate of ERAS overexpressing neuroblastoma cells when exposed to common chemotherapeutic agents (Aoyama, 2010). It has been suggested that the higher survival rate is mediated through the ERAS-PI3K pathway, since the survival rate has decreased in the presence of a selective PI3K inhibitor. The ERAS overexpressing cell lines have shown higher levels of phosphorylated AKT in the immunoblot-analysis as compared to the parental cell lines. ERAS overexpression, however, has not changed the amount of phosphorylated ERK, a downstream effector of the MAPK pathway. Furthermore, increased colony formation of the ERAS overexpressing cells was observed. In conclusion, the presence of ERAS does not promote proliferation, but facilitates transforming activity of cells, indicating that ERAS rather takes role in the process of transformation to malignant cells (Aoyama, 2010). In 2010, Kubota et al. have investigated the role of ERAS in tumorgenicity of human gastric cancer, not only by including cell lines, but also gastric cancer tissues (Kubota, et al., 2010). This group have conducted an immunohistochemically staining with an anti *hs*ERAS-antibody and found out that the expression of ERAS is quite heterogenous. The expression, however, did not correlate to the differentiation grade, but interestingly was associated with liver and lymph node metastasis. PCR array analysis then showed that ERAS suppresses the expression E-cadherin mRNA. They have proposed that ERAS overexpression induces EMT since the mRNA levels of the E-cadherin repressors, such as *ZFHX1A*, *ZFHX1B* and *TCF3*, have significantly increased. Furthermore, ERAS overexpressing cell lines have shown stronger formation of colonies,

while knockdown of ERAS inhibited the cell invasion. Collectively, ERAS may have transforming activity in gastric cancer, which is associated with tumor progression and metastasis (Kubota et al., 2010).

So far ERAS has been assumed to have transforming activity and to play a role in progression of cancer cells. In 2013, Wei and colleagues investigated the effects of ERAS on the cell proliferation. Therefore, two gastric cancer cell lines, endogenously expressing ERAS, were treated with ERAS siRNA, and have shown that ERAS knockdown has resulted in inhibition of cell proliferation. They have proposed a role of ERAS in proliferation, which is different from the study published by Kubota et al. (Wei, 2013).

5.5 Proposed function of endogenous ERAS in Teratocarcinoma cells

In the context of this work, we found out that *hs*ERAS is strongly expressed in the teratocarcinoma cell lines, leading back to the very first report of *hs*ERAS in 2003, where Takahashi et al. have identified ERAS as a new member of the RAS family (Takahashi, Mitsui, & Yamanaka, 2003). This group found ERAS in undifferentiated embryonic cells of mice. They have initially elucidated the phenomenon of teratoma formation when transplanting embryonic stem cells. They have generated a stably ERAS expressing NIH3T3 cell population and a stably HRASV12 expressing cell population. In both settings morphological changes have been observed, indicating that both proteins induce transformation of the cells. However, analyses revealed that HRASV12 promotes tumorgenicity via transformation of the cells through a mechanism different to ERAS. While HRASV12 induced premature senescence, ERAS increased growth rate. However, according to Takahashi and coworkers ERAS is not necessary for the maintenance of pluripotency of ESC (Takahashi, Mitsui, & Yamanaka, 2003).

More recently, the group of Yu have analyzed the role of ERAS in stimulation of somatic cell reprogramming (Yu et al., 2014). This group has overexpressed ERAS in OG-MEF cells by performing retroviral transduction and has also transduced cells with vectors fused to GFP coding for Oct4, Sox2 and K1f4. The cells have then been cultured under conditions for mouse iPSC induction. They have reported that ERAS enhances iPSC induction by 10-fold and significantly increases the expression of key pluripotency genes (Nanog, Oct4 and Esrrb). A decrease of reprogramming efficiency has been observed when endogenous ERAS was knocked down by shRNA transduction. They have proposed that ERAS-AKT-FoxO1 signaling pathway is crucial for cell reprogramming and carcinogenesis (Yu et al., 2014).

In 2015, Kwon et al. have shown that ERAS overexpressing fibroblasts show increased proliferation due to an increased phospho-JNK levels, upregulated cyclin D and E, and G1/S transition (Kwon et al., 2015). They proposed that ERAS facilitates cell reprogramming through accelerated cell cycle progression, mediated by ERAS-JNK pathway (Kwon et al., 2015).

Collectively, ERAS appears to regulate the expression of pluripotency genes (Yu, et al., 2014) and cell cycle progression (Kwon, et al., 2015), and so is critical for cell reprogramming and also carcinogenesis. Interestingly, the teratocarcinoma cell lines showed the highest levels of ERAS mRNA in the present study. This cell lines are known to develop from teratomas, which are commonly known to be pluripotent, and share properties with stem cells. This opens an interesting link to ERAS and carcinogenesis.

Chapter 6 Outlook

This thesis showed for the first time the expression of ERAS in several cancer-entities in human cancer cell lines. It shows the expression of ERAS at the mRNA level and points out that the expression at the protein level is probably very low, impeding the detection of the protein itself.

To conclude whether the attendance of ERAS is part of the carcinogenesis, further investigations are needed to be performed. Inclusive a more sensitive method to detect even the lowest amounts of a protein. Once this hurdle is overcome, further investigations, such as analysis of the described cell signaling pathways, using a cancer cell line, which is highly expressing ERAS, are required. In this context a lentiviral knock-down of ERAS could serve as a control.

Chapter 7

References

Ahmadian, M. R., Hoffmann, U., Goody, R. S., & Wittinghofer, A. (1997). Individual rate constants for the interaction of Ras proteins with GTPase-activating proteins determined by fluorescence spectroscopy. *Biochemistry, 36*(15), 4535-4541. doi: 10.1021/bi962556y

Andrews, P. W. (2002). From teratocarcinomas to embryonic stem cells. *Philos Trans R Soc Lond B Biol Sci, 357*(1420), 405-417. doi: 10.1098/rstb.2002.1058

Aoyama. (2010). Resistance to chemotherapeutic agents and promotion of transforming activity mediated by embryonic stem cell-expressed Ras (ERas) signal in neuroblastoma cells. *International Journal of Oncology, 37*(4). doi: 10.3892/ijo_00000752

ATCC, CAPAN-1. https://www.lgcstandards-atcc.org/products/all/HTB-79.aspx [03.07.2019, 10:24]

ATCC, CAPAN-2. https://www.lgcstandards-atcc.org/products/all/HTB-80.aspx [03.07.2019, 10:30]

ATCC, MIAPaCa-2. https://www.lgcstandards-atcc.org/products/all/CRL-1420.aspx [03.07.2019, 10:40]

ATCC, HT-29. https://www.lgcstandards-atcc.org/products/all/HTB-38.aspx#characteristics [03.07.2019, 11:10]

ATCC, IMR-32. https://www.lgcstandards-atcc.org/products/all/CCL-127.aspx [03.07.2019, 11:55]

ATCC, LoVo. https://www.lgcstandards-atcc.org/products/all/CCL-229.aspx [03.07.2019, 11:12]

ATCC, NCCIT. https://www.lgcstandards-atcc.org/products/all/CRL-2073.aspx#generalinformation [03.07.2019, 11:35]

ATCC, NTERA-2. https://www.lgcstandards-atcc.org/products/all/CRL-1973.aspx [03.07.2019, 11:42]

ATCC, SH-SY5Y. https://www.lgcstandards-atcc.org/products/all/CRL-2266.aspx#characteristics [03.07.2019, 11:59]

ATCC, SW480. https://www.lgcstandards-atcc.org/products/all/CCL-228.aspx#characteristics [03.07.2019, 11:16]

ATCC, Tera-1. https://www.lgcstandards-atcc.org/products/all/HTB-105.aspx [03.07.2019, 11:37]

ATCC, Tera-2. https://www.lgcstandards-atcc.org/products/all/HTB-106.aspx [03.07.2019, 11:40]

Balkwill, F., Charles, K. A., & Mantovani, A. (2005). Smoldering and polarized inflammation in the initiation and promotion of malignant disease. Cancer Cell, 7(3), 211-217.

Barrett, J. C. (1993). Mechanisms of multistep carcinogenesis and carcinogen risk assessment. Environ Health Perspect, 100, 9-20.

Bertram, J. S. (2000). The molecular biology of cancer. *Mol Aspects Med, 21*(6), 167-223.

Bishop, A. L., & Hall, A. (2000). Rho GTPases and their effector proteins. Biochem J, 348 Pt 2, 241-255.

Bos, J. L. (1989). ras oncogenes in human cancer: a review. *Cancer Res, 49*(17), 4682-4689.

Bourne, H. R., Sanders, D. A., & McCormick, F. (1991). The GTPase superfamily: conserved structure and molecular mechanism. Nature, 349(6305), 117-127. doi: 10.1038/349117a0

Bray, Freddie. (2014). Transitions in human development and the global cancer burden. In Bernard W. Stewart & Christopher P. Wild (Eds.), *World Cancer Report 2014* (pp. 54-68). Lyon: International Agency for Research on Cancer.

Buday, László, & Downward, Julian. (2008). Many faces of Ras activation. Biochimica et Biophysica Acta (BBA) - Reviews on Cancer, 1786(2), 178-187. doi: 10.1016/j.bbcan.2008.05.001

Buhrman, G., Kumar, V. S. S., Cirit, M., Haugh, J. M., & Mattos, C. (2010). Allosteric Modulation of Ras-GTP Is Linked to Signal Transduction through RAF Kinase. Journal of Biological Chemistry, 286(5), 3323-3331. doi: 10.1074/jbc.M110.193854

Carrier, F., Georgel, P. T., Pourquier, P., Blake, M., Kontny, H. U., Antinore, M. J., . . . Fornace, A. J., Jr. (1999). Gadd45, a p53-responsive stress protein, modifies DNA accessibility on damaged chromatin. Mol Cell Biol, 19(3), 1673-1685.

Castellano, E., & Santos, E. (2011). Functional Specificity of Ras Isoforms: So Similar but So Different. Genes & Cancer, 2(3), 216-231. doi: 10.1177/1947601911408081

Cho, K. J., Park, J. H., Piggott, A. M., Salim, A. A., Gorfe, A. A., Parton, R. G., . . . Hancock, J. F. (2012). Staurosporines disrupt phosphatidylserine trafficking and mislocalize Ras proteins. J Biol Chem, 287(52), 43573-43584. doi: 10.1074/jbc.M112.424457

Cirstea, I. C., Gremer, L., Dvorsky, R., Zhang, S. C., Piekorz, R. P., Zenker, M., & Ahmadian, M. R. (2013). Diverging gain-of-function mechanisms of two novel KRAS mutations associated with Noonan and cardio-facio-cutaneous syndromes. Hum Mol Genet, 22(2), 262-270. doi: 10.1093/hmg/dds426

Cirstea, I. C., Kutsche, K., Dvorsky, R., Gremer, L., Carta, C., Horn, D., . . . Zenker, M. (2010). A restricted spectrum of NRAS mutations causes Noonan syndrome. Nat Genet, 42(1), 27-29. doi: 10.1038/ng.497

Coleman, Mathew L., Marshall, Christopher J., & Olson, Michael F. (2004). RAS and RHO GTPases in G1-phase cell-cycle regulation. Nature Reviews Molecular Cell Biology, 5(5), 355-366. doi: 10.1038/nrm1365

COSMIC, CAPAN-1. https://cancer.sanger.ac.uk/cosmic/sample/overview?id=1761694 [03.07.2019, 10:49]

COSMIC, CAPAN-2. https://cancer.sanger.ac.uk/cosmic/sample/overview?id=1299297 [03.07.2019, 10:50]

COSMIC, HCTT-116. https://cancer.sanger.ac.uk/cosmic/sample/overview?id=1998442 [03.07.2019, 11:07]

COSMIC, LoVo. https://cancer.sanger.ac.uk/cosmic/sample/overview?id=1945867 [03.07.2019, 11:14]

COSMIC, SW480. https://cancer.sanger.ac.uk/cosmic/sample/overview?id=2302018 [03.07.2019, 11:18]

DSMZ, BPH-1. https://www.dsmz.de/collection/catalogue/details/culture/ACC-143 [03.07.2019, 11:20]

Flex, E., Jaiswal, M., Pantaleoni, F., Martinelli, S., Strullu, M., Fansa, E. K., . . . Tartaglia, M. (2014). Activating mutations in RRAS underlie a phenotype within the

RASopathy spectrum and contribute to leukaemogenesis. Hum Mol Genet. doi: 10.1093/hmg/ddu148

Gradiz, R., Silva, H. C., Carvalho, L., Botelho, M. F., & Mota-Pinto, A. (2016). MIA PaCa-2 and PANC-1 - pancreas ductal adenocarcinoma cell lines with neuroendocrine differentiation and somatostatin receptors. *Sci Rep, 6*, 21648. doi: 10.1038/srep21648srep21648 [pii]

Gremer, L., Merbitz-Zahradnik, T., Dvorsky, R., Cirstea, I. C., Kratz, C. P., Zenker, M., . . . Ahmadian, M. R. (2011). Germline KRAS mutations cause aberrant biochemical and physical properties leading to developmental disorders. Hum Mutat, 32(1), 33-43. doi: 10.1002/humu.21377

Hanahan, D., & Weinberg, R. A. (2000). The hallmarks of cancer. *Cell, 100*(1), 57-70.

Hanahan, D., & Weinberg, R. A. (2011). Hallmarks of cancer: the next generation. Cell, 144(5), 646-674. doi: 10.1016/j.cell.2011.02.013

He, L., & Hannon, G. J. (2004). MicroRNAs: small RNAs with a big role in gene regulation. *Nat Rev Genet, 5*(7), 522-531.

Hollstein, M., Sidransky, D., Vogelstein, B., & Harris, C. C. (1991). p53 mutations in human cancers. Science, 253(5015), 49-53.

Iwauchi, Takehiko, Tanaka, Hiroaki, Yamazoe, Sadaaki, Yashiro, Masakazu, Yoshii, Mami, Kubo, Naoshi, . . . Hirakawa, Kosei. (2011). Identification of HLA-A*2402-restricted epitope peptide derived from ERas oncogene expressed in human scirrhous gastric cancer. *Cancer Science, 102*(4), 683-689. doi: 10.1111/j.1349-7006.2010.01843.x

Kaizaki, R., Yashiro, M., Shinto, O., Yasuda, K., Matsuzaki, T., Sawada, T., & Hirakawa, K. (2009). Expression of ERas oncogene in gastric carcinoma. *Anticancer Res, 29*(6), 2189-2193. doi: 29/6/2189 [pii]

Kameda, Takashi, & Thomson, James A. (2005). HumanERasGene Has an Upstream Premature Polyadenylation Signal That Results in a Truncated, Noncoding Transcript. *Stem Cells, 23*(10), 1535-1540. doi: 10.1634/stemcells.2005-0054

Kleinsmith, L. J., & Pierce, G. B., Jr. (1964). Multipotentiality of Single Embryonal Carcinoma Cells. *Cancer Res, 24*, 1544-1551.

Kordes, Claus, & Häussinger, Dieter. (2013). Hepatic stem cell niches. Journal of Clinical Investigation, 123(5), 1874-1880. doi: 10.1172/jci66027

Kubota, E., Kataoka, H., Aoyama, M., Mizoshita, T., Mori, Y., Shimura, T., . . . Joh, T. (2010). Role of ES cell-expressed Ras (ERas) in tumorigenicity of gastric cancer. *Am J Pathol, 177*(2), 955-963. doi: 10.2353/ajpath.2010.091056

Kwon, Y. W., Jang, S., Paek, J. S., Lee, J. W., Cho, H. J., Yang, H. M., & Kim, H. S. (2015). E-Ras improves the efficiency of reprogramming by facilitating cell cycle progression through JNK-Sp1 pathway. *Stem Cell Res, 15*(3), 481-494. doi: 10.1016/j.scr.2015.09.004

Lane, D. P. *Cancer. p53, guardian of the genome*: Nature. 1992 Jul 2;358(6381):15-6.

Liotta, L. A., & Stetler-Stevenson, W. G. (1991). Tumor invasion and metastasis: an imbalance of positive and negative regulation. Cancer Res, 51(18 Suppl), 5054s-5059s.

Liu, Y., Yin, T., Feng, Y., Cona, M. M., Huang, G., Liu, J., . . . Ni, Y. (2015). Mammalian models of chemically induced primary malignancies exploitable for imaging-based preclinical theragnostic research. *Quant Imaging Med Surg, 5*(5), 708-729. doi: 10.3978/j.issn.2223-4292.2015.06.01qims-05-05-708 [pii]

Malkin, D., Li, F. P., Strong, L. C., Fraumeni, J. F., Jr., Nelson, C. E., Kim, D. H., . . . et al. (1990). Germ line p53 mutations in a familial syndrome of breast cancer, sarcomas, and other neoplasms. Science, 250(4985), 1233-1238.

Nakhaei-Rad, S., Nakhaeizadeh, H., Gotze, S., Kordes, C., Sawitza, I., Hoffmann, M. J., . . . Ahmadian, M. R. (2016). The Role of Embryonic Stem Cell-expressed RAS (ERAS) in the Maintenance of Quiescent Hepatic Stellate Cells. *J Biol Chem, 291*(16), 8399-8413.

Nakhaei-Rad, S., Nakhaeizadeh, H., Kordes, C., Cirstea, I. C., Schmick, M., Dvorsky, R., . . . Ahmadian, M. R. (2015). The function of embryonic stem cell-expressed Ras (E-Ras), a unique Ras family member, correlates with its additional motifs and its structural properties. *J Biol Chem*. doi: 10.1074/jbc.M115.640607

Omerovic, J., Laude, A. J., & Prior, I. A. (2007). Ras proteins: paradigms for compartmentalised and isoform-specific signalling. Cellular and Molecular Life Sciences, 64(19-20), 2575-2589. doi: 10.1007/s00018-007-7133-8

Papke, B., & Der, C. J. (2017). Drugging RAS: Know the enemy. *Science, 355*(6330), 1158-1163.

Peltomaki, P. (2012). Mutations and epimutations in the origin of cancer. Exp Cell Res, 318(4), 299-310.

Potenza, Nicoletta, Vecchione, Carmine, Notte, Antonella, De Rienzo, Assunta, Rosica, Annamaria, Bauer, Lisa, . . . Di Lauro, Roberto. (2005). Replacement of K-Ras with H-Ras supports normal embryonic development despite inducing cardiovascular pathology in adult mice. EMBO reports, 6(5), 432-437. doi: 10.1038/sj.embor.7400397

Protter, D. S., & Parker, R. (2016). Principles and Properties of Stress Granules. *Trends Cell Biol, 26*(9), 668-679.

Public Health England, PNT2. https://www.phe-culturecollections.org.uk/products/celllines/generalcell/detail.jsp?refId=95012613&collection=ecacc_gc [03.07.2019, 11:32]

Pylayeva-Gupta, Yuliya, Grabocka, Elda, & Bar-Sagi, Dafna. (2011). RAS oncogenes: weaving a tumorigenic web. *Nature Reviews Cancer, 11*(11), 761-774. doi: 10.1038/nrc3106

Repasky, G. A., Chenette, E. J., & Der, C. J. (2004). Renewing the conspiracy theory debate: does Raf function alone to mediate Ras oncogenesis? Trends Cell Biol, 14(11), 639-647. doi: 10.1016/j.tcb.2004.09.014

Riede, Ursus-Nikolaus, Werner, Martin, & Freudenberg, Nikolaus. (2009). Basiswissen Allgemein und Spezielle Pathologie. Heidelberg: Springer.

Scheffzek, K., Ahmadian, M. R., Kabsch, W., Wiesmuller, L., Lautwein, A., Schmitz, F., & Wittinghofer, A. (1997). The Ras-RasGAP complex: structural basis for GTPase activation and its loss in oncogenic Ras mutants. Science, 277(5324), 333-338.

Scheidig, A. J., Burmester, C., & Goody, R. S. (1999). The pre-hydrolysis state of p21(ras) in complex with GTP: new insights into the role of water molecules in the GTP hydrolysis reaction of ras-like proteins. Structure, 7(11), 1311-1324.

Siegel, R. L., Miller, K. D., & Jemal, A. (2019). Cancer statistics, 2019. *CA Cancer J Clin, 69*(1), 7-34. doi: 10.3322/caac.21551

Schmick, Malte, Vartak, Nachiket, Papke, Björn, Kovacevic, Marija, Truxius, Dina C, Rossmannek, Lisaweta, & Bastiaens, Philippe I H. (2014). KRas Localizes to the

Plasma Membrane by Spatial Cycles of Solubilization, Trapping and Vesicular Transport. Cell, 157(2), 459-471. doi: 10.1016/j.cell.2014.02.051

Takahashi, K., Mitsui, K., & Yamanaka, S. (2003). Role of ERas in promoting tumour-like properties in mouse embryonic stem cells. *Nature, 423*(6939), 541-545. doi: 10.1038/nature01646nature01646 [pii]

Takahashi, K., Murakami, M., & Yamanaka, S. (2005). Role of the phosphoinositide 3-kinase pathway in mouse embryonic stem (ES) cells. Biochem Soc Trans, 33(Pt 6), 1522-1525. doi: 10.1042/bst20051522

Takahashi, K., & Yamanaka, S. (2006). Induction of pluripotent stem cells from mouse embryonic and adult fibroblast cultures by defined factors. Cell, 126(4), 663-676.

Tanaka, Y., Ikeda, T., Kishi, Y., Masuda, S., Shibata, H., Takeuchi, K., . . . Hanazono, Y. (2009). ERas is expressed in primate embryonic stem cells but not related to tumorigenesis. *Cell Transplant, 18*(4), 381-389. doi: 10.3727/096368909788809794

Thomson, J. A., Itskovitz-Eldor, J., Shapiro, S. S., Waknitz, M. A., Swiergiel, J. J., Marshall, V. S., & Jones, J. M. (1998). Embryonic stem cell lines derived from human blastocysts. Science, 282(5391), 1145-1147.

Vogelstein, B., & Kinzler, K. W. (1993). The multistep nature of cancer. Trends Genet, 9(4), 138-141.

Waters, A. M., & Der, C. J. (2018). KRAS: The Critical Driver and Therapeutic Target for Pancreatic Cancer. *Cold Spring Harb Perspect Med, 8*(9). doi: a031435 [pii]10.1101/cshperspect.a031435cshperspect.a031435 [pii]

Wei, Fang. (2013). Role of the ERas gene in gastric cancer cells. *Oncology Reports*. doi: 10.3892/or.2013.2417

Weinberg, Robert A. (2014). *The Biology of Cancer* (2nd edition ed.): Garland Science, Taylor & Francis Group, LLC.

Wennerberg, K. (2005). The Ras superfamily at a glance. Journal of Cell Science, 118(5), 843-846. doi: 10.1242/jcs.01660

Wittinghofer, Alfred, & Vetter, Ingrid R. (2011). Structure-Function Relationships of the G Domain, a Canonical Switch Motif. Annual Review of Biochemistry, 80(1), 943-971. doi: 10.1146/annurev-biochem-062708-134043

Yashiro. (2009). Epigenetic regulation of the embryonic oncogene ERas in gastric cancer cells. *International Journal of Oncology, 35*(05). doi: 10.3892/ijo_00000414

Yasuda, K., Yashiro, M., Sawada, T., Ohira, M., & Hirakawa, K. (2007). ERas oncogene expression and epigenetic regulation by histone acetylation in human cancer cells. *Anticancer Res, 27*(6B), 4071-4075.

Yin, Chunyue, Evason, Kimberley J., Asahina, Kinji, & Stainier, Didier Y. R. (2013). Hepatic stellate cells in liver development, regeneration, and cancer. Journal of Clinical Investigation, 123(5), 1902-1910. doi: 10.1172/jci66369

Yu, Y., Liang, D., Tian, Q., Chen, X., Jiang, B., Chou, B. K., . . . Wang, G. (2014). Stimulation of somatic cell reprogramming by ERas-Akt-FoxO1 signaling axis. *Stem Cells, 32*(2), 349-363. doi: 10.1002/stem.1447

Yuspa, S. H., & Poirier, M. C. (1988). Chemical carcinogenesis: from animal models to molecular models in one decade. Adv Cancer Res, 50, 25-70

Chapter 8

Acknowledgements

First of all, I want to express my sincere thanks to Prof. Dr. Reza Ahmadian for the opportunity to work in his group. Furthermore, I would like to thank him for his support, and his time. Reza, thank you very much for opening the door to scientific work for me.

A special thank to Saeideh Nakhaei-Rad for your supervision, your advice, your help, but also for your friendship and companionship. It means more to me than words can tell.

In addition, I want to express my gratitude to the Ahmadian group members: Dr. Ehsan Amin, Marcel Buchholzer, Dr. Fereshteh Haghighi, Dr. Jana Lissy, Dr. Hossein Nakhaeizadeh and Dr. Kazem Nouri.

I Also want to thank Dr. Alexander Lang for supporting me and telling me over and over again: “This is science”!

Thanks to PD Roland Piekorz, for every discussion, the help you offered me, your advice and the support.

Special thanks to all of the members of the Institute of Biochemistry and Molecular Biology II at the medical department of the Heinrich-Heine-University, for the opportunity to be part of the group as well as for your help.

Furthermore, I owe my deepest gratitude to Dr. Nikolas Stoecklein, Prof. Dr. Wolfgang Schulz and Prof. Dr. Guido Reifenberger for providing the cell lines for my work.

Last but not least, I want to thank my family, my friends and Patrick Markus Kleine without whose support and patience I could not have done this work.

Andrews, P. W. (2002). From teratocarcinomas to embryonic stem cells. *Philos Trans R Soc Lond B Biol Sci, 357*(1420), 405-417. doi: 10.1098/rstb.2002.1058

Bray, Freddie. (2014). Transitions in human development and the global cancer burden. In Bernard W. Stewart & Christopher P. Wild (Eds.), *World Cancer Report 2014* (pp. 54-68). Lyon: International Agency for Research on Cancer.

Gradiz, R., Silva, H. C., Carvalho, L., Botelho, M. F., & Mota-Pinto, A. (2016). MIA PaCa-2 and PANC-1 - pancreas ductal adenocarcinoma cell lines with neuroendocrine differentiation and somatostatin receptors. *Sci Rep, 6*, 21648. doi: 10.1038/srep21648

srep21648 [pii]

Liu, Y., Yin, T., Feng, Y., Cona, M. M., Huang, G., Liu, J., . . . Ni, Y. (2015). Mammalian models of chemically induced primary malignancies exploitable for imaging-based preclinical theragnostic research. *Quant Imaging Med Surg, 5*(5), 708-729. doi: 10.3978/j.issn.2223-4292.2015.06.01

qims-05-05-708 [pii]

Siegel, R. L., Miller, K. D., & Jemal, A. (2019). Cancer statistics, 2019. *CA Cancer J Clin, 69*(1), 7-34. doi: 10.3322/caac.21551

Waters, A. M., & Der, C. J. (2018). KRAS: The Critical Driver and Therapeutic Target for Pancreatic Cancer. *Cold Spring Harb Perspect Med, 8*(9). doi: a031435 [pii]

10.1101/cshperspect.a031435

cshperspect.a031435 [pii]

Weinberg, Robert A. (2014). *The Biology of Cancer* (2nd edition ed.): Garland Science, Taylor & Francis Group, LLC.